Dynamical viscosity of nucleating bubbles

S. Alamoudi,[1] D. G. Barci,[2] D. Boyanovsky,[1] C. A. A. de Carvalho,[3] E. S. Fraga,[3] S. E. Jorás,[3] and F. I. Takakura[4]
[1]*Department of Physics and Astronomy, University of Pittsburgh, Pittsburgh, Pennsylvania 15260*
[2]*Instituto de Física, Universidade Estadual do Rio de Janeiro, Rio de Janeiro, RJ, 20559-900, Brazil*
[3]*Instituto de Física, Universidade Federal do Rio de Janeiro, C.P. 68528, Rio de Janeiro, RJ, 21945-970 Brazil*
[4]*Departamento de Física, Instituto de Ciências Exatas, Universidade Federal de Juiz de Fora, Juiz de Fora, MG, 36036-330, Brazil*
(Received 19 April 1999; published 1 November 1999)

We study the viscosity corrections to the growth rate of nucleating bubbles in a slightly supercooled first order phase transition in (1+1)- and (3+1)-dimensional scalar field theory. We propose a *microscopic* approach that leads to the nonequilibrium equation of motion of the coordinate that describes small departures from the critical bubble and allows us to extract the growth rate consistently in a weak coupling expansion and in the thin wall limit. Viscosity effects arise from the interaction of this coordinate with the stable quantum and thermal fluctuations around a critical bubble. In the case of $1+1$ dimensions we provide an estimate for the growth rate that depends on the details of the free energy functional. In $3+1$ dimensions we recognize robust features that are a direct consequence of the thin wall approximation that transcend a particular model. These are long-wavelength hydrodynamic fluctuations that describe surface waves. We identify these low energy modes with quasi Goldstone modes which are related to surface waves on interfaces in phase ordered Ising-like systems. In the thin wall limit the coupling of this coordinate to these hydrodynamic modes results in the largest contribution to the viscosity corrections to the growth rate. For a ϕ^4 scalar field theory at temperature $T<T_c$, the growth rate to lowest order in the quartic self-coupling λ is $\Omega=(\sqrt{2}/R_c)[1-0.003\lambda T\xi(R_c/\xi)^2]$ with R_c,ξ the critical radius and the width of the bubble wall, respectively. We obtain the effective non-Markovian Langevin equation for the radial coordinate and derive the generalized fluctuation dissipation relation. The noise is correlated on time scales Ω^{-1} as a result of the coupling to the slow hydrodynamic modes. We discuss the applicability of our results to describe the growth rate of hadron bubbles in a quark-hadron first order transition. [S0556-2821(99)07120-9]

PACS number(s): 11.27.+d, 05.70.Fh, 12.38.Mh

I. INTRODUCTION

The dynamics of first order phase transitions is a fundamental ingredient in particle physics and in condensed matter. First order phase transitions occur via the nucleation of bubbles of the true vacuum phase in the metastable or false vacuum phase. At large temperature it is mediated by thermal or overbarrier activation and at low temperatures via quantum nucleation. First order phase transitions are conjectured to occur in QCD and in electroweak theory. In QCD a first order phase transition *could* describe the hadronization of the quark-gluon plasma, possibly produced in the early Universe at about 10^{-5} s after the big bang or in relativistic heavy ion collisions [1–3]. In electroweak theory a first order phase transition is argued to provide the nonequilibrium setting for baryogenesis [4–6]. In early universe cosmology, first order phase transitions had been proposed as mechanisms to generate the inflationary stage [7–9]. In condensed matter physics thermal activation results in the nucleation of bubbles of the lowest free energy phase in binary fluids [10,11] and also of the decay of metastable dimerized states in quasi-one-dimensional charge density wave systems and nondegenerate organic conductors [12,13].

The most comprehensive microscopic theory of nucleation via thermal activation was presented by Langer [14] and was later extended to quantum field theory to account both for thermal activation as well as for quantum nucleation [15–18]. An approach to describe nucleation in a nonsteady state situation in real time has been advocated in Ref. [19]. In the limit in which nucleation is dominated by thermal activation and overbarrier transitions, these bubbles are produced via large thermal fluctuations. These bubbles will grow whenever their radius is larger than a critical value and collapse if it is smaller. Supercritical bubbles will grow to convert the metastable phase into the stable phase or until they percolate achieving the total conversion of the metastable phase. For slightly supercritical bubbles an important *dynamical* quantity is the growth rate of a bubble

$$\Omega=\frac{d}{dt}\left[\ln\left|\frac{R(t)}{R_c}-1\right|\right];\quad R(t)\geqslant R_c \tag{1.1}$$

with $R(t)$ the (time dependent) radius of a slightly supercritical nucleating bubble and R_c is the critical radius [14,3,10]. Langer's theory provides the nucleation rate per unit volume per unit time given by

$$I=\Omega\mathcal{D}e^{-F_b/T} \tag{1.2}$$

where F_b is the free energy of a critical bubble and $\mathcal{D}$ is proportional to the ratio of the determinants of the fluctuation operators around the bubble configuration to that around the homogeneous metastable state [14,3,10]. The regime of applicability of homogeneous nucleation theory is for $F_b\gg T$, for $F_b\approx T$ small amplitude thermal fluctuations can trigger the phase transition and nucleation and spinodal decomposition can no longer be distinguished. The ratio of determinants in $\mathcal{D}$ has been computed analytically and numerically

in several important cases [20–22]. Csernai and Kapusta [3] have studied the growth rate of hadronic bubbles in a quark gas by extending Langer's theory to the relativistic case. These authors studied a coarse-grained field theory in terms of a relativistic hydrodynamic description with viscous terms in the energy momentum tensor and the baryon current. Their conclusion was that the growth rate is determined by the coefficients of the shear and bulk viscosities and that hadronic bubbles do not grow when these coefficients vanish. Another approach presented by Ruggeri and Friedman [23] also based on baryon-free relativistic hydrodynamics but with a different treatment of the heat conduction and energy flow reached a different conclusion, th at the growth rate is nonzero even for vanishing bulk and shear viscosities and that viscosity effects are subleading for small viscosities. If the hadronization phase transition is of first order there are potentially important experimental signatures associated with the homogeneous nucleation of the hadronic phase some of which had been studied in Ref. [24].

Homogeneous nucleation of the quark-gluon plasma has been recently studied with a bag model of the equation of state for the quark and hadron phases and the different predictions above have been compared [25]. The formulation and results of Csernai and Kapusta had recently been used to study first order quark-hadron phase transition in the early Universe for a first order hadronization transition [26] and more recently homogeneous nucleation has been tested numerically in $(2+1)$-dimensional systems with qualitative agreement to the standard result [27].

An alternative phenomenological description of the growth rate based on dissipative hydrodynamics combined with the finite temperature effective potential has been presented in Ref. [28]. In this work analytical and numerical studies reveal a dependence of the growth rate on the phenomenological dissipative coefficient.

Khlebnikov [29] and Arnold [30] have studied dissipative effects that slow down the growth rate of a supercritical bubble by coupling the order parameter that describes nucleation to *other fields* (with a trilinear coupling) and applied the fluctuation dissipation relation to one loop order in the coupling to the other field.

Finally we must mention a numerical approach to the description of nucleation, based on a phenomenological Markovian Langevin dynamics in terms of the finite temperature effective potential (typically computed to one loop order) with a (local) friction coefficient and a Gaussian white noise term related by the fluctuation-dissipation theorem [31,32]. The use of the finite temperature effective potential in the description of the inhomogeneous bubble configuration that seeds the nucleation of the phase of lowest free energy is an important ingredient, in particular in coarse-grained phenomenological descriptions [3]. Finite temperature effects are included in the coarse grained free energy which describes long wavelength physics by integrating out short wavelength fluctuations which are in thermodynamic equilibrium [33,34]. These finite temperature corrections modify quantitatively and sometimes substantially the equilibrium free energy functional, for example, the position of the minima, masses, and couplings. These are important parameters that determine the profile of the bubble configuration, since the asymptotic behavior of the bubble is determined by the position of the minima of the equilibrium free energy.

The importance of the growth rate for describing the dynamics of nucleation in the hadronization and the electroweak phase transitions as well as the practical importance of nucleation in quasi-one-dimensional organic conductors justifies a continued effort to understand from a *microscopic* perspective the influence of dissipation, viscosity, and friction upon the growth rate of supercritical nucleating bubbles.

Focus and strategy. Our goal in this article is precisely to study dissipative effects upon the growth rate Ω from a more *microscopic* point of view in model quantum field theories that describe the main features of nucleation. The simplest model to study nucleation and a first order phase transition is a ϕ^4 field theory with a small explicit symmetry breaking term that breaks the degeneracy between ground states and thus leads to the existence of a metastable state. Although arguably this model could hardly describe the features of the quark-hadron or electroweak phase transitions, our hope is to extract robust phenomena that will be generic to the physics of nucleation and that could enlighten the effect of viscosity on the growth rate.

This study begins by identifying the inhomogeneous bubble configuration which is a solution of the static equations of motion. We include the finite temperature effects by considering the equation of motion in terms of the finite temperature effective potential, this is achieved consistently by the addition of finite temperature counterterms to the Lagrangian. The quadratic fluctuations around this bubble solution feature an unstable mode that describes small perturbations from the critical bubble. The instability is a manifestation of the growth (or collapse) of supercritical (or subcritical) bubbles and the unstable eigenvalue is directly related to the growth rate of slightly supercritical bubbles. In addition to this unstable mode there are modes of zero frequency corresponding to translations of this configuration and modes of positive frequency that correspond to stable fluctuations.

The main strategy is to consider the dynamics of the coordinate that determines the unstable direction in functional space, and treating it as a collective coordinate. We then focus on the *interaction* of this coordinate with those representing the stable fluctuations by expanding the original Lagrangian in terms of these coordinates in function space and recognize the interaction terms between these coordinates. The translational mode is anchored and ignored since we are not interested in studying the dynamics of the translational degree of freedom but that of the growth of a supercritical bubble. We assume that the stable degrees of freedom are in thermal equilibrium and that they serve as a ''bath'' with which the unstable coordinate interacts. Integrating out the degrees of freedom associated with the stable fluctuations we obtain an effective description of the dynamics for the unstable coordinate which includes the ''viscosity and friction'' effects associated with the transfer of energy to the stable modes. This description allows us to obtain the equations of motion for the expectation value of the unstable coordinate wherefrom we can obtain the corrections to the growth rate

from the interaction with the stable degrees of freedom. Furthermore, integrating out the stable degrees of freedom in the nonequilibrium functional allows us to extract the effective Langevin equation for the unstable coordinate and to obtain consistently the noise terms. We emphasize that this approach is *fundamentally different* from the previous studies described above. First of all, we are *not* computing the ratio of determinants that enter in the rate expression. This ratio of determinants only involves the quadratic fluctuations but *not* the interaction between the coordinates associated with the fluctuations. Our approach is different from that of Refs. [29,30], in these references the coupling of the order parameter associated with the nucleating field was to *other independent fields*. Contrary to this we consider the coupling of the unstable coordinates to the stable fluctuations involving the *same* field. Our approach starts from the microscopic theory and does not rely on a hydrodynamic description, however, as it will be seen later, long-wavelength hydrodynamic fluctuations associated with surface waves provide the largest contribution to viscosity effects in three spatial dimensions.

In a very specific sense our program obtains the effective action for the degree of freedom that represents departures from a critical bubble by integrating out the degrees of freedom describing stable fluctuations, but of the *same field*. Our approach must necessarily rely on several different approximations: (i) weak coupling to allow a perturbative expansion of the effective action and the real time equations of motion, (ii) the thin wall approximation in which the critical radius is much larger than the width of the bubble wall. This approximation is necessary to be able to provide quantitative answers. Finally as it will be justified later the important fluctuations can be described by the *classical* limit of the finite temperature distribution functions.

We carry out this program to lowest order in the quartic coupling and to leading order in the thin wall approximation both in $1+1$ and $3+1$ dimensions. The motivation to study the lower-dimensional case is provided by its potential application in experimentally relevant condensed matter systems [12,13].

Summary of results. Our main results can be summarized as a consistent perturbative correction to the growth rate from ''dynamical viscosity'' effects associated with the interaction of the radius of the bubble with the stable quantum and thermal fluctuations. In $1+1$ dimensions the growth rate for bubbles is given by Eq. (3.15) with R_c, ξ the radius and width of the critical bubble, respectively, λ the quartic self-coupling, and $F[R_c/\xi]$ a slowly varying dimensionless function that depends on the details of the potential and spectrum of stable fluctuations, in particular scattering states.

In $3+1$ dimensions we find that in the thin wall limit the important low energy excitations are *hydrodynamic fluctuations* associated with surface waves. These are identified as quasiGoldstone bosons and give the dominant contribution to viscosity effects on the growth rate. These low energy excitations are a robust feature of *any* model and not particular to the one considered in this article, however, the *coupling* of the unstable radial coordinate to these fluctuations depends on the model. To lowest order in the coupling the growth rate is given by Eq. (4.40). Furthermore, we obtain the effective Langevin equation for the unstable coordinate that reveals the correct microscopic correlations of the noise term showing that the coupling to the hydrodynamic modes determine that the noise is correlated on time scales Ω^{-1}.

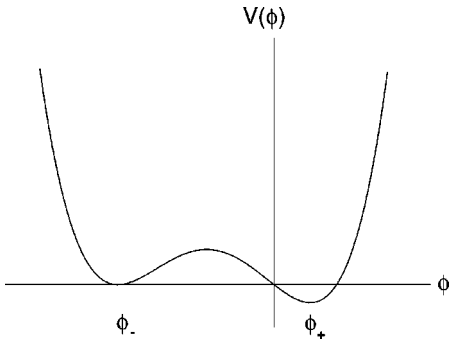

FIG. 1. Form of the potential $V(\phi)$.

The article is organized as follows. Section II introduces the model, describes the strategy in detail, and sets up the general form of the correction to the growth rate to lowest order (one loop) and in the classical limit. In Sec. III the case of $1+1$ dimensions is analyzed in detail within the model considered. In Sec. IV we study the $(3+1)$-dimensional case, and discuss the low energy fluctuations associated with surface waves, providing the argument that these are quasiGoldstone hydrodynamic fluctuations. We argue that these low energy fluctuations are present independent of the model and will dominate the viscosity corrections to the growth rate. The conclusions are presented in Sec. V, along with a critical discussion on the validity of our results to describe the growth rate of supercritical bubbles in coarse-grained descriptions of a first order quark-hadron phase transition. An appendix presents the effective Langevin equation for small departures of the critical radius and analyzes the generalized fluctuation-dissipation relation.

II. THE MODEL: GENERALITIES AND STRATEGY

We consider a real scalar field $\phi(x)$ whose dynamics is determined by the following Lagrangian density:

$$\mathcal{L}=\frac{1}{2}(\partial_\mu\phi)(\partial^\mu\phi)-V(\phi), \tag{2.1}$$

where $V(\phi)$ is a double well potential with a metastable minimum at ϕ_- and a stable minimum at ϕ_+. It proves convenient to parametrize it in the following form:

$$V(\phi)=\lambda(\phi-\phi_-)^2\phi(\phi-\phi^*). \tag{2.2}$$

This form of the potential is depicted in Fig. 1 and is very similar to the coarse-grained free energy proposed in Ref. [3] identifying the local energy variable e in that reference with the scalar field ϕ, and also similar to the effective potential description used in numerical simulations for electroweak theory [31,32,34].

The stable minimum ϕ_+ is given by

$$\phi_+ = \frac{1}{8}(2\phi_- + 3\phi_* - \sqrt{4\phi_-^2 + 9\phi_*^2 - 4\phi_-\phi_*}), \quad (2.3)$$

where the point ϕ_* is parametrized by the mass m of small oscillations around the *metastable* minimum ϕ_- as

$$\phi^* \equiv \phi_-(1-\epsilon), \quad (2.4)$$

where

$$\epsilon \equiv \frac{m^2}{2\lambda\phi_-^2} \quad \text{and} \quad m^2 \equiv V''(\phi_-) \quad (2.5)$$

and λ is the quartic coupling. Although this parametrization does not look familiar it will prove advantageous later. In particular, $(1-\epsilon)$ gives a measure of the free energy difference between the true and the false vacua and is therefore related to the supercooling temperature. As $\epsilon \to 1$, the two minima become degenerate and the condition $\epsilon \approx 1$ defines the thin-wall limit (this will become clear later when we analyze the bubble profile), when the radius of the nucleating bubble is much larger than the width of its surface ξ (or the correlation length). This corresponds to the case of small supercooling $T < T_c$ but $T/T_c \approx 1$ in the description of Ref. [3]. In the thin wall limit, we find that ϕ_+ has the following simple form:

$$\phi_+ = -\frac{\phi_-}{2}(\epsilon - 1) + \mathcal{O}[(\epsilon - 1)^2]. \quad (2.6)$$

A. The counterterms

We anticipate that there will be renormalization of the parameters in the potential, not only arising from ultraviolet divergences but more importantly from medium effects, i.e., finite temperature contributions to the mass, couplings and explicit symmetry breaking terms. In particular in three spatial dimensions we expect a correction to the mass and the linear symmetry breaking term both proportional to $T^2, T, \ldots$. The origin of these finite temperature corrections are the usual tadpole diagrams, the correction to the linear symmetry breaking term is a consequence of the trilinear coupling. These finite temperature corrections are the usual ones obtained in an effective potential description and provide a finite renormalization to the potential. Our aim is to describe the dynamical aspects of the thermal fluctuations that are responsible for thermal activation and the nucleation of the true phase in the false vacuum phase. These are the solutions of the static field equations but *in presence of the thermal fluctuations*, i.e., with the potential renormalized by the finite temperature effects. That is to say, the potential that must enter in the field equations must be the finite temperature effective potential [27,31–34]. The finite temperature effective potential includes the finite temperature corrections for static and homogeneous field configurations. Including these finite temperature effects in the equations of motion guarantees that the *inhomogeneous* bubble configurations will asymptotically tend to the homogeneous values of the field representing the *correct* extrema of the equilibrium free energy. Furthermore, these finite temperature renormalizations will determine the *correct* scales for the bubble size, its width and the unstable frequency associated with the growth of a supercritical bubble.

We account for these finite temperature renormalizations by replacing the parameters in the potential by the finite temperature renormalized parameters and adding counterterms to the Lagrangian. The counterterms are then found consistently in a coupling or loop expansion by requesting that they cancel the contributions from the tadpole (or similar) terms *completely*, i.e., including the finite temperature parts. This prescription is at the heart of using the finite temperature effective potential to study the solutions that lead to the decay of the metastable state [3,27,31–34]. Thus the Lagrangian density becomes

$$\mathcal{L}[\phi] = \frac{1}{2}(\partial_\mu\phi)(\partial^\mu\phi) - V(\phi,T) + \delta\mathcal{L}_{ct}[\phi], \quad (2.7)$$

where the potential $V(\phi,T)$ is of the same form as in Eq. (2.2) but in terms of the parameters that include the finite temperature (and ultraviolet) renormalizations, i.e., $\lambda(T), m(T), \epsilon(T)$, etc. and the counterterm Lagrangian density is of the form

$$\delta\mathcal{L}_{ct} = \delta\lambda\,\phi^4 + \delta g\,\phi^3 + \delta M^2\phi^2 + H\phi, \quad (2.8)$$

where space-time translational invariance dictates that the counterterms are constant. These counterterms will be consistently chosen in the loop expansion to cancel the contribution from local tadpoles. We will argue below that this procedure renormalizes consistently in perturbation theory the *static* properties of the bubble, in particular the width and radius of a critical bubble. In particular the free energy density studied in [3,31–34] is precisely of this form with parameters that depend on temperature.

At this point we may consider adding to the counterterms a wave-function renormalization which would involve corrections for inhomogeneous configurations. A wave-function renormalization will arise at one loop order and beyond because of the trilinear coupling. However, computing this correction in the usual loop expansion around a homogeneous background is not very relevant for the bubble configuration. Since our goal is to obtain the *real time* equations of motion for particular fluctuations around the bubble configuration, these renormalizations will arise automatically in the equations of motion obtained to one loop order. Thus the counterterms that we include in the Lagrangian density are only those for *static* renormalization thus accounting for the correct scales and asymptotic values of the classical solution and obtain the equivalent of the wave-function renormalization directly from the real time evolution of fluctuations around the bubble configuration. This procedure will become clear when we obtain explicitly the evolution equations in the next sections.

We will focus our attention on the cases of one and three spatial dimensions. Although the case of one spatial dimension is of limited interest in particle physics, it is important in condensed matter and statistical physics of quasi-one-

dimensional systems [12,13]. Furthermore most aspects of the treatment are general and the one-dimensional case provides a somewhat simpler setting to introduce the main strategy as well as to explore the general features. The three-dimensional case will be studied in detail subsequently.

B. The bubbles

Before proceeding to the specific situations, we now consider general features of the bubble solutions and the quadratic fluctuations around them to focus on the precise strategy to follow. A critical bubble is a solution of the *static* field equations, which in terms of the (effective) potential $V(\phi,T)$ is given in one spatial dimension by

$$-\frac{d^2\phi_b}{dx^2}+\left.\frac{\partial V(\phi,T)}{\partial\phi}\right|_{\phi_b}=0 \tag{2.9}$$

with boundary conditions such that $\phi_b\to\phi_-$ for $|x|\to\infty$. Such a solution describes a ''bubblelike'' configuration which approaches the false vacuum at asymptotically large distances and probes the true vacuum in a localized region in space of size $2R_c$ with R_c the critical ''radius.'' Such a solution will be found in detail in Sec. III. In three spatial dimensions, the critical bubble is a radially symmetric static field configuration solution of the following equation

$$-\frac{d^2\phi_b}{dr^2}-\frac{2}{r}\frac{d\phi_b}{dr}+\left.\frac{\partial V(\phi,T)}{\partial\phi}\right|_{\phi_b}=0 \tag{2.10}$$

with the boundary condition $\phi_b(r)\to\phi_-$ as $r\to\infty$. It corresponds to a field configuration that starts close to the true vacuum ϕ_+ and tends to the false vacuum ϕ_- at asymptotically large radial distance. The solution of Eq. (2.10) will be studied in detail in the thin wall approximation in Sec. IV.

In both cases the change from the true vacuum to the false one occurs around the radius of the bubble R_c over a distance $\xi(T)\sim 1/m$ that defines the wall thickness of the bubble and is related to the correlation length in the metastable phase. We will study the nonequilibrium dynamical viscosity of nucleating bubbles in the thin wall limit in which the radius of the bubble is much larger than the wall thickness; i.e., $R\gg\xi$. These field configurations are parametrized by two important coordinates: $\vec{x}_0$ which describes the position of the center of the bubble and the radius R, i.e., a bubble configuration is of the form $\phi(\vec{x}-\vec{x}_0;R)$ and a critical bubble corresponds to $R=R_c$ determined by the solution to the equations of motion (2.9),(2.10). The coordinate $\vec{x}_0$ is associated with translational invariance and typically treated as a collective coordinate [35], while the radius R determines the size of the bubble and will be treated also as a collective coordinate (see below). Since we are not concerned here with the dynamics of the translational degrees of freedom, but rather with that of the radius, we ''clamp'' the collective coordinate $\vec{x}_0$ by fixing the center of the bubble at $\vec{x}_0=0$. Integration over this collective coordinate results in the typical volume factor [14,15] and is not relevant for our discussion.

In d space dimensions, we can use the radius of the bubble R as a variational parameter and introduce the total energy of a bubble configuration with radius R by

$$E_{\rm var}(R)=\int d^dx\left[\frac{1}{2}[\nabla\phi_b(\vec{x},R)]^2+V[\phi_b(\vec{x},R)]\right]. \tag{2.11}$$

and in the limit $R/\xi(T)\gg 1$ (thin wall) has two main contributions: a volume contribution proportional to R^d which is negative and arises from the region of the bubble that probes the true vacuum which has lower (free) energy, and a surface term which is positive and arises from the region of the bubble corresponding to the wall, includes gradient terms and is therefore proportional to the area of the surface of the wall R^{d-1}. In one spatial dimension the ''surface'' of the bubble corresponds to two points and the gradient energy saturates to a constant independent of the radius for large bubble radius.

The general behavior of the total energy of a bubble configuration as a function of $s=R/\xi$ is depicted in Fig. 3 for one spatial dimension and in Fig. 4 for three spatial dimensions (see Secs. III and IV). The maximum of the energy function determines the value of the critical radius R_c as discussed in detail in the next sections. Clearly a critical bubble is an *unstable* static solution of the equations of motion. For $R<R_c$ the surface energy term dominates and the bubble shrinks into the false vacuum phase, for $R>R_c$ the volume energy dominates and the bubble will grow as the gain in the volume energy is greater than the cost in elastic surface energy.

A more clear description is obtained in the case of three spatial dimensions for a spherically symmetric bubble. Let σ be the surface tension (energy per unit area) of the spherical bubble configuration separating the metastable phase from the stable one. Then the total energy of the bubble is

$$E_{\rm var}(R)=-\frac{4\pi}{3}\Delta\mathcal{F}R^3+4\pi\sigma R^2+\cdots, \tag{2.12}$$

where $\Delta\mathcal{F}=|V(\phi_+,T)-V(\phi_-,T)|$, and the dots stand for corrections that are subleading in the thin wall approximation, see Sec. IV [Eq. (4.22) for details]. These (small) corrections will be neglected for the arguments presented below. The energy attains its maximum E_c at the critical radius

$$R_c=\frac{2\sigma}{\Delta\mathcal{F}} \tag{2.13}$$

and it is given by

$$E_c\equiv E_{\rm var}(R_c)=\frac{4\pi\sigma}{3}R_c^2=\frac{16\pi\sigma^3}{3(\Delta\mathcal{F})^2}. \tag{2.14}$$

Near the maximum of the energy function, it can be written as an expansion in terms of the (small) departures from the critical radius as

$$E_{\rm var}(R)=E_c-\frac{1}{2}\omega^2(R-R_c)^2+\cdots, \tag{2.15}$$

where the frequency

$$-\omega^2\equiv\left.\frac{d^2E_{\rm var}(R)}{dR^2}\right|_{R_c}=-8\pi\sigma \tag{2.16}$$

is independent of the critical radius and $\Delta\mathcal{F}$ and as it will be seen in detail below, it is related to the growth rate of slightly supercritical bubbles.

C. Fluctuations

The study of the fluctuations around the classical bubble configuration begins by studying the spectrum of the fluctuation operator

$$\left[-\frac{d^2}{dx^2}+V''[\phi_b(x,R_c)]\right]\mathcal{U}_n(x)=\omega_n^2\mathcal{U}_n(x)F \quad \text{in 1D}, \tag{2.17}$$

$$\{-\vec{\nabla}^2+V''[\phi_b(\vec{x},R_c)]\}\mathcal{U}_n(\vec{x})=\omega_n^2\mathcal{U}_n(\vec{x}) \quad \text{in 3D}, \tag{2.18}$$

where the prime represents differentiation with respect to the field ϕ. Taking a spatial derivative of the equation of motion satisfied by the bubble configuration it is straightforward to find that

$$\mathcal{U}_0(x,R_c)\propto\frac{d\phi_b(x,R_c)}{dx} \tag{2.19}$$

is a solution of the one dimensional eigenvalue problem (2.17) with $\omega_0^2=0$ and that

$$\mathcal{U}_0(\vec{x},R_c)\propto\frac{\vec{x}}{|\vec{x}|}\frac{d\phi_b(r,R_c)}{dr} \tag{2.20}$$

are eigenfunctions of the three-dimensional fluctuation operator with zero eigenvalue. These are the zero modes arising from translational invariance [14,15,35]. In one dimension the zero mode is an odd function of x since the bubble solution is even, therefore it has a node. Hence there must be another solution of the Schrödinger-like operator (2.17) that has no nodes and has a smaller and therefore *negative* eigenvalue. The form of the bubble solution in the thin wall approximation is that of a widely separated kink-antikink pair, as it will be shown in detail in the next section we find that the eigenfunction corresponding to the negative eigenvalue must be $\mathcal{U}_{-1}\propto d\phi_b(x,R)/dR|_{R_c}$. This can be understood simply from the fact that the zero mode associated with the bubble solution is the *antisymmetric* combination of the zero modes associated with the individual kinks [35], hence the eigenfunction with lower eigenvalue must be the *symmetric* combination and the form of the bubble profile immediately leads to the conclusion that is the derivative with respect to the radius [see Sec. III, Eq. (3.11)]. In the three-dimensional case, the zero modes (2.20) correspond to the angular momentum $l=1$ spherical harmonics, therefore there must be an $l=0$ (spherically symmetric) solution of the Schrödinger-like eigenvalue problem (2.18) with a *negative eigenvalue*. In a later section we study in detail the bubble solution and the spectrum of fluctuations around it and conclude that the eigenfunction corresponding to the negative eigenvalue is $\mathcal{U}_{-1}\propto d\phi_b(r,R)/dR|_{R_c}$ in the thin wall approximation [see Sec. IV, Eq. (4.27) for $\mathcal{U}_{000}$].

Therefore the respective spectra of the fluctuation operators are

$$\mathcal{U}_{-1}(\vec{x},R_c)=\sqrt{N_{-1}}\left.\frac{d\phi(\vec{x},R)}{dR}\right|_{R_c},$$

$$\omega_{-1}^2=-\Omega^2;\quad \Omega^2>0;$$

$$\mathcal{U}_0(\vec{x},R_c)=\sqrt{N_0}\vec{\nabla}\phi(\vec{x},R_c),\quad \omega_0^2=0,$$

$$\mathcal{U}_{n>0}(\vec{x},R_c),\quad \omega_n^2>0, \tag{2.21}$$

with $N_{-1};N_0$ normalization factors (chosen real). The classical bubble solution corresponds to a saddle point in functional space, the mode $\mathcal{U}_{-1}$ determines an unstable direction.

The field operator can now be expanded in the complete basis of eigenfunctions of (2.17),(2.18) in either case and write in general

$$\phi(\vec{x},t)=\phi_b(\vec{x}-\vec{x}_0,R_c)+q_{-1}(t)\mathcal{U}_{-1}(\vec{x}-\vec{x}_0)+q_0(t)\mathcal{U}_0(\vec{x}-\vec{x}_0)+\sum_{n>0}q_n(t)\mathcal{U}_n(\vec{x}-\vec{x}_0), \tag{2.22}$$

whereas the bound state eigenfunctions are chosen real, the scattering states are chosen to satisfy the hermiticity condition $\mathcal{U}_n(\vec{x})=\mathcal{U}_{-n}^*(\vec{x})$; $q_n(t)=q_{-n}^*(t)$. The quanta associated with the coordinates $q_{n>0}$ for the stable modes will be referred generically as ''mesons,'' and the operators $q_{n>0}$ create and annihilate meson states.

From Eq. (2.21) it is clear that the modes $\mathcal{U}_0;\mathcal{U}_{-1}$ correspond to shifts in the position of the bubble, $\vec{x}_0$ and the radius R, respectively. The collective coordinate treatment [35] absorbs the zero mode $\mathcal{U}_0$ into a definition of a new quantum mechanical degree of freedom $\hat{\vec{x}}_0(t)$ and expands the field operator in terms of the directions perpendicular to this zero mode,

$$\phi(\vec{x},t)=\phi_b[\vec{x}-\hat{\vec{x}}_0(t),R_c]+q_{-1}(t)\mathcal{U}_{-1}[\vec{x}-\hat{\vec{x}}_0(t)]+\sum_{n>0}q_n(t)\mathcal{U}_n[\vec{x}-\hat{\vec{x}}_0(t)]. \tag{2.23}$$

We are not interested in the dynamics of the translational collective coordinate, therefore we will ''clamp'' the position of the bubble and focus solely on the dynamics of the unstable coordinate $q_{-1}(t)$. Technically this is achieved by

inserting a functional delta function for $\hat{\vec{x}}_0(t)$ in the path integral, the corresponding Jacobian from the change of field variables to the collective coordinate [35] leads to the usual volume factor [14,15], hence in what follows we will set $\hat{\vec{x}}_0(t)=0$. We note that for small amplitudes of the unstable mode we can write the expansion (2.23) as

$$\phi(\vec{x},t)\approx\phi_b[\vec{x},R(t)]+\sum_{n>0} q_n(t)\mathcal{U}_n(\vec{x});$$

$$R(t)=R_c+q_{-1}(t)\sqrt{N_{-1}} \tag{2.24}$$

that allows us to identify $R(t)-R_c=q_{-1}(t)\sqrt{N_{-1}}$ and the coordinate q_{-1} is associated with small departures from the critical radius.

D. The relation between Ω^2 and ω^2

At this stage we recognize that the fluctuation mode $\mathcal{U}_{-1}(\vec{x})\propto d\phi_b(\vec{x},R_c)/dR_c$ is the (unstable) functional direction along which the bubble either grows or collapses, therefore the coordinate $q_{-1}(t)\propto[R(t)-R_c]$ describes the small fluctuations around the critical bubble. An immediate question is, what is the relation between the frequency ω^2 in Eqs. (2.15),(2.16) and Ω^2, the eigenvalue associated with $\mathcal{U}_{-1}$ (2.21)? The answer to this important question is obtained by taking the second derivative of the total energy in Eq. (2.11) with respect to the radius of the bubble R, which results in the following equation:

$$\frac{d^2E_{\rm var}(R)}{dR^2}=\int d^dr\left\{\left[\vec{\nabla}\left(\frac{d\phi_b}{dR}\right)\right]^2+\vec{\nabla}\phi_b.\vec{\nabla}\left(\frac{d^2\phi_b}{dR^2}\right)+\left(\frac{d^2\phi_b}{dR^2}\right)\frac{\partial V(\phi_b)}{\partial\phi}+\left(\frac{d\phi_b}{dR}\right)^2\frac{\partial^2V(\phi_b)}{\partial\phi^2}\right\}. \tag{2.25}$$

Integrating the first two terms in Eq. (2.25) by parts using the boundary conditions for the bubble solution and Eqs. (2.9),(2.10),(2.17),(2.18), which are evaluated at the critical radius R_c, we obtain the following relation:

$$\left.\frac{d^2E_{\rm var}(R)}{dR^2}\right|_{R=R_c}=-\omega^2=-\frac{\Omega^2}{N_{-1}} \tag{2.26}$$

in terms of the normalization factor of the unstable mode [see Eq. (2.21)] which will be found for the one and three-dimensional cases separately below. We note that the relation (2.24) determines that in the absence of interactions with other degrees of freedom the growth rate of a supercritical bubble is given by

$$\frac{d}{dt}\left[\ln\left|\frac{R(t)}{R_c}-1\right|\right]=\Omega \tag{2.27}$$

for small departures from the critical radius.

Equation (2.26) is very useful since it relates the second derivative of the total *classical* variational energy $E_{\rm var}(R)$ (the energy of the classical bubble as a function of its radius) to the eigenfrequency associated with the *quantum* unstable mode. Usually it is a difficult task to find the spectrum of the quantum fluctuation operator, and consequently the frequency of the unstable mode. The above relation can be used to find the value of the unstable frequency, or the normalization factor N_{-1} if the frequencies are known.

E. The strategy

Our goal is to study the effects of quantum and thermal fluctuations upon the *real time* evolution of a bubble whose radius is slightly larger than critical. This is achieved by treating the coordinate $q_{-1}(t)\propto[R(t)-R_c]$ as a *collective coordinate*, i.e., the radius of the bubble is treated as a fully quantum mechanical variable interacting with the other degrees of freedom corresponding to the stable fluctuations and described by the coordinates $q_n(t)$. The ''zero mode'' (translational degree of freedom) is clamped and frozen since we are only interested in describing the dynamics of the unstable mode. The interaction of the stable degrees of freedom with the collective coordinate describing the departure from the critical radius will introduce viscosity effects and slow down the growth of a supercritical bubble. This will result in a smaller growth rate and our aim is to precisely compute this viscosity effect on the growth rate for small departures from the critical radius. By including the finite temperature *static* counterterms in the Lagrangian and requesting that these be cancelled consistently in the perturbative expansion, we can isolate the static renormalization to the unstable frequency from the *dynamical* viscosity effects associated with the energy transfer to the stable modes.

This program begins by expanding the field in terms of the unstable and stable coordinates (after clamping the translational mode) as

$$\phi(x,t)=\phi_b(x,R_c)+q_{-1}(t)\mathcal{U}_{-1}(x)+\sum_p q_p(t)\mathcal{U}_p(x), \tag{2.28}$$

where the summation index p runs over all stable, bound, and scattering states other than the translational and unstable modes. Throughout the index p refers to both scattering and bound states.

Using the above expansion, Eq. (2.28), of the field $\phi(x,t)$, the Lagrangian can be shown to have the following form:

$$L[q_{-1},q_p]=L_0[q_{-1}]+L_0[q_p]+L_I[q_{-1},q_p], \tag{2.29}$$

where

$$L_0[q_{-1}]=\frac{1}{2}\{\dot{q}^2_{-1}(t)+\Omega^2q^2_{-1}(t)+\delta\Omega^2_{ct}q^2_{-1}(t)+hq_{-1}(t)\}, \tag{2.30}$$

$$L_0[q_p]=\frac{1}{2}\sum_p \{\dot{q}_p(t)\dot{q}_{-p}(t)-\omega_p^2 q_p(t)q_{-p}(t)\}, \tag{2.31}$$

$$\begin{aligned} L_I[q_{-1},q_p]=&-\sqrt{\lambda}q_{-1}(t)\sum_{p,p'}\mathcal{B}_{pp'}q_p(t)q_{p'}(t)-q_{-1}^2(t)\\ &\times\left\{\sqrt{\lambda}\sum_p \mathcal{B}_p q_p(t)+\lambda\sum_{p,p'}\mathcal{A}_{pp'}q_p(t)q_{p'}(t)\right\}\\ &-q_{-1}^3(t)\left\{\sqrt{\lambda}\mathcal{B}_{-1}+\lambda\sum_p \mathcal{A}_p q_p(t)\right\}\\ &-\lambda\mathcal{A}_{-1}q_{-1}^4(t)+\text{h.o.t}+L_{ct}[q_{-1},q_p], \end{aligned} \tag{2.32}$$

where we have used the equations of motion satisfied by the bubble configurations, and Eqs. (2.17) and (2.18). The terms $\delta\Omega_{ct}^2 q_{-1}^2; hq_{-1}$ are the quadratic and linear terms in q_{-1} from the counterterm Lagrangian. The terms denoted by h.o.t. in Eq. (2.32) correspond to higher order interactions that are not important to the order that we are studying. The term $L_{ct}[q_{-1},q_p]$ arise from the nonlinear (cubic and higher) terms in the coordinates from the counterterm Lagrangian, they do not need to be specified since they will be requested to cancel tadpole and static terms in the equations of motion for the collective coordinate q_{-1} and do not contribute to lowest order $[\mathcal{O}(\lambda)]$. The matrix elements are given by

$$\begin{aligned} \mathcal{B}_{pp'}\equiv&\frac{1}{2\sqrt{\lambda}}\int_{-\infty}^{+\infty}dx'\mathcal{U}_{-1}(x')\mathcal{U}_p(x')\mathcal{U}_{p'}(x')\\ &\times V'''[\phi_b(x',R_c)], \end{aligned} \tag{2.33}$$

$$\mathcal{B}_p\equiv\frac{1}{2\sqrt{\lambda}}\int_{-\infty}^{+\infty}dx'\mathcal{U}_{-1}^2(x')\mathcal{U}_p(x')V'''[\phi_b(x',R_c)], \tag{2.34}$$

$$\mathcal{B}_{-1}\equiv\frac{1}{6\sqrt{\lambda}}\int_{-\infty}^{+\infty}dx'\mathcal{U}_{-1}^3(x')V'''[\phi_b(x',R_c)], \tag{2.35}$$

$$\mathcal{A}_{pp'}\equiv 6\int_{-\infty}^{+\infty}dx'\mathcal{U}_{-1}^2(x')\mathcal{U}_p(x')\mathcal{U}_{p'}(x'), \tag{2.36}$$

$$\mathcal{A}_p\equiv 4\int_{-\infty}^{+\infty}dx'\mathcal{U}_{-1}^3(x')\mathcal{U}_p(x'), \tag{2.37}$$

$$\mathcal{A}_{-1}\equiv\int_{-\infty}^{+\infty}dx'\mathcal{U}_{-1}^4(x'), \tag{2.38}$$

so that the λ dependence is explicit in each term of the effective action.

We thus see that the above Lagrangian describes a quantum mechanical degree of freedom q_{-1} interacting with a bath of infinitely many degrees of freedom q_p, as well as with self-interaction. The self-interaction of the coordinate q_{-1} will be neglected because we are only interested in the viscosity effects arising from interaction with the stable degrees of freedom. The nonlinear terms in q_{-1} are neglegted because we will extract the growth rate for small departures from the critical bubble.

The bath of mesons will introduce viscosity effects on evolution of the coordinate associated with departures from the critical radius and will result in a correction to the growth rate. These effects can be studied in a consistent manner by integrating out the meson degrees of freedom in a consistent perturbative expansion, thus obtaining the nonequilibrium effective action for q_{-1}. The variational derivative of this effective action leads to the equation of motion that includes the effects of the meson bath. This nonequilibrium effective action is obtained up to one loop order in Appendix B. The effective equation of motion is a Langevin equation with a non-Markovian viscosity kernel and a Gaussian noise term (to one loop order) whose correlations are related to the viscosity kernel via the fluctuation-dissipation relation. The details are provided in Appendix B. Alternatively we obtain the equation of motion for the expectation value of the coordinate q_{-1} directly by means of linear response.

We have already accounted for the *static* renormalization of the unstable frequency Ω by introducing the finite temperature counterterms and using the finite temperature effective potential in the equations of motion. However, we anticipate that there will arise further corrections to the growth rate Ω from *velocity dependent* terms in the effective equations of motion. These are truly *dynamical* viscosity effects which cannot be captured by a static calculation. The viscosity terms that are a function of the time derivative of the unstable coordinate will be revealed by obtaining the effective nonequilibrium equation of motion for this coordinate by integrating out the stable modes, which act as a bath for the quantum mechanical degree of freedom q_{-1}. We will restrict our study to small departures from the critical radius and obtain the linearized equation of motion for the expectation value of q_{-1}. This is consistent with the definition of the growth rate as the logarithmic derivative of the radius for small departures from the critical value. As is clear from Eq. (2.30), in the absence of interactions the Hamiltonian for the unstable coordinate q_{-1} is that of an *inverted harmonic oscillator* (of negative frequency squared) and small departures from the unstable equilibrium value $q_{-1}=0$ will grow exponentially with the growth rate Ω.

F. The initial value problem

We study the time evolution of the expectation value of the unstable coordinate $Q=\langle q_{-1}\rangle$ by proposing an initial state described by a density matrix which is a tensor product of the density matrix for the unstable coordinate and a density matrix that describes all the stable modes in thermal equilibrium at a given temperature. Therefore

$$\rho(0)=\rho_{-1}(0)\otimes\rho_s(0), \tag{2.39}$$

where ρ_{-1} describes a pure state in which the expectation value of the unstable coordinate is Q_0, and $\rho_s(0)$ is a thermal density matrix for the stable modes. As mentioned above the translational mode is clamped. The time evolution of the initially prepared density matrix is given by Liouville's equation, whose solution is

$$\rho(t)=U(t)\rho(0)U^{-1}(t) \tag{2.40}$$

with $U(t)$ being the unitary time evolution operator. As described in detail in Ref. [36] the time evolution can be cast in terms of a time dependent Hamiltonian in which the interaction is switched on at the initial time $t=0$. Alternatively the initial value problem can be cast in terms of linear response to an external source adiabatically turned on from $t=-\infty$ that determines the initial preparation [37]. Both approaches are equivalent and the reader is referred to Refs. [36,37] for more details on the initial value problem.

The equation of motion in real time is obtained by using the generating functional of nonequilibrium Green's functions which requires a path integral along a contour in complex time and the following effective Lagrangian [38,39]:

$$L_{\rm eff}=L[q^{+}_{-1},q^{+}_{p}]-L[q^{-}_{-1},q^{-}_{p}], \tag{2.41}$$

where the labels $\pm$ refer to the forward (+) and backward (-) branches along the complex time contour [38,39]. The equation of motion for the expectation value $Q(t)=\langle q_{-1}(t)\rangle$ is obtained by performing the shift

$$q^{\pm}_{-1}(t)=Q(t)+\tilde{q}^{\pm}(t); \quad \langle\tilde{q}^{\pm}(t)\rangle=0. \tag{2.42}$$

Imposing the condition $\langle\tilde{q}^{\pm}(t)\rangle=0$ to all orders in perturbation theory leads to the retarded equation of motion for $Q(t)$. For a detailed presentation of this method in many other situations see Ref. [39].

The important ingredients in this program are the real time Green's functions for the stable coordinates which are assumed to be in thermal equilibrium. These are the following:

$$\begin{aligned}\langle q^{+}_{p}(t)q^{+}_{p'}(t')\rangle&=-i\delta_{p,-p'}G^{++}_{p}(t,t')\\&=-i\delta_{p,-p'}[\mathcal{G}^{>}_{p}(t,t')\Theta(t-t')\\&\quad+\mathcal{G}^{<}_{p}(t,t')\Theta(t'-t)],\end{aligned}$$

$$\begin{aligned}\langle q^{-}_{p}(t)q^{-}_{p'}(t')\rangle&=-i\delta_{p,-p'}G^{--}_{p}(t,t')\\&=-i\delta_{p,-p'}[\mathcal{G}^{>}_{p}(t,t')\Theta(t'-t)\\&\quad+\mathcal{G}^{<}_{p}(t,t')\Theta(t-t')],\end{aligned}$$

$$\langle q^{+}_{p}(t)q^{-}_{p'}(t')\rangle=i\delta_{p,-p'}G^{+-}_{p}(t,t')=-i\delta_{p,-p'}\mathcal{G}^{<}_{p}(t,t'),$$

$$\begin{aligned}\langle q^{-}_{p}(t)q^{+}_{p'}(t')\rangle&=i\delta_{p,-p'}G^{-+}_{p}(t,t')\\&=-i\delta_{p,-p'}\mathcal{G}^{>}_{p}(t,t')=-i\delta_{p,-p'}\mathcal{G}^{<}_{p}(t',t),\end{aligned} \tag{2.43}$$

where

$$\begin{aligned}\mathcal{G}^{>}_{p}(t,t')&=\frac{i}{2\omega_p}[(1+n_p)\exp\{-i\omega_p(t-t')\}\\&\quad+n_p\exp\{i\omega_p(t-t')\}],\end{aligned}$$

$$\begin{aligned}\mathcal{G}^{<}_{p}(t,t')&=\frac{i}{2\omega_p}[(1+n_p)\exp\{i\omega_p(t-t')\}\\&\quad+n_p\exp\{-i\omega_p(t-t')\}],\end{aligned}$$

$$n_p=\frac{1}{\exp\{\beta\omega_p\}-1}. \tag{2.44}$$

We will carry our derivation of the equation of motion in the linear theory where we will neglect nonlinear terms, $\mathcal{O}(Q^2)$ and higher, and furthermore we will neglect the self-interaction of the unstable coordinate (cubic and quartic terms). As mentioned before, the linearization of the equation of motion is consistent with the focus on the dissipative corrections to the growth rate, which is defined for small departures from the critical radius. In this case, the nonequilibrium effective action $S_{\rm eff}$ becomes

$$\begin{aligned}S_{\rm eff}=\int_{-\infty}^{+\infty}dt\Big\{&L_0[\tilde{q}^{+}(t)]+L_0[q^{+}_{p}(t)]+\tilde{q}^{+}(t)\\&\times\Big[-\ddot{Q}(t)+(\Omega^2+\delta\Omega^2_{ct})Q(t)\\&-\sqrt{\lambda}\,\theta(t)\sum_{p,p'}\mathcal{B}_{p,p'}q^{+}_{p}(t)q^{+}_{p'}(t)\\&-2\lambda\,\theta(t)\sum_{p,p'}\mathcal{A}_{p_1p_2}q^{+}_{p_1}(t)q^{+}_{p_2}(t)Q(t)+h\Big]\\&-\sqrt{\lambda}\,\theta(t)Q(t)\sum_{p,p'}\mathcal{B}_{pp'}q^{+}_{p}(t)q^{+}_{p'}(t)-[(+)\leftrightarrow(-)]\Big\},\end{aligned} \tag{2.45}$$

where we have written only the terms that are relevant to the lowest order calculation $\mathcal{O}(\lambda)$ which is the focus of the present discussion and included the time dependence of the Hamiltonian to set up the initial value problem [36].

Imposing the condition $\langle\tilde{q}^{+}_{-1}(t)\rangle=0$, up to $\mathcal{O}(\lambda)$, we obtain the following equation to one-loop order:

$$i\int_{-\infty}^{\infty}dt'\langle\tilde{q}^{+}(t)\tilde{q}^{+}(t')\rangle\Big[\ddot{Q}(t')-\Omega^{2}Q(t')-\Delta Q(t')$$
$$-\mathcal{H}-2i\lambda\sum_{p_1,p_2,p_3,p_4}\mathcal{B}_{p_1p_2}\mathcal{B}_{p_3p_4}$$
$$\times\int_{-\infty}^{+\infty}dt''\{\langle q^{+}_{p_1}(t')q^{+}_{p_3}(t'')\rangle\langle q^{+}_{p_2}(t')q^{+}_{p_4}(t'')\rangle$$
$$-\langle q^{+}_{p_1}(t')q^{-}_{p_3}(t'')\rangle\langle q^{+}_{p_2}(t')q^{-}_{p_4}(t'')\rangle\}Q(t'')\Big]$$
$$=0$$

with

$$\Delta=\delta\Omega^{2}_{ct}-2\lambda\sum_{p,p'}\mathcal{A}_{p,p'}\langle q^{+}_{p}(t')q^{+}_{p'}(t')\rangle,$$

$$\mathcal{H}=h-\sqrt{\lambda}\sum_{p,p'}\mathcal{B}_{p,p'}\langle q^{+}_{p}(t')q^{+}_{p'}(t')\rangle. \tag{2.46}$$

Since the correlation $\langle\tilde{q}^{+}(t)\tilde{q}^{+}(t')\rangle$ does not vanish for all values of t and t', this implies that the quantity between the square brackets must vanish [39]. Furthermore, we now choose the counterterm in such a way to ensure that $\mathcal{H}=0$. We thus obtain the equation of motion for the expectation value of the unstable coordinate for $t>0$

$$\ddot{Q}(t)-\Omega^{2}Q(t)-\Delta Q(t)-\lambda\int_{0}^{t}dt'\Sigma(t-t')Q(t')=0;$$
$$\dot{Q}(t=0)=0;\quad Q(t=0)=Q_0, \tag{2.47}$$

where the self-energy $\Sigma(t-t')$ is given by

$$\Sigma(t-t')=\sum_{p,p'}\frac{|\mathcal{B}_{pp'}|^{2}}{\omega_p\omega_{p'}}\{(1+n_p+n_{p'})\sin[(\omega_p+\omega_{p'})(t-t')]$$
$$-(n_p-n_{p'})\sin[(\omega_p-\omega_{p'})(t-t')]\}, \tag{2.48}$$

and we have used the fact that $\mathcal{B}^{*}_{p,p'}=\mathcal{B}_{-p,-p'}$. The two different terms in the self-energy, proportional to the sum and difference of frequencies respectively have a simple but important interpretation. The first term proportional to the sum of frequencies corresponds to the process in which the coordinate q_{-1} ''decays'' into two mesons with probability $(1+n_p)(1+n_{p'})$ minus the ''recombination'' process with probability $n_pn_{p'}$. The second term proportional to the difference of frequencies originates in Landau damping and corresponds to the scattering of the unstable coordinate with mesons in the medium, with probability $(1+n_{p'})n_p$ minus the reverse process with probability $(1+n_p)n_{p'}$ [40]. The counterterm $\delta\Omega^{2}_{ct}$ will be chosen to cancel the tadpole contribution to Δ [see Eq. (2.46)] as well as the *static* contribution from the self-energy, since this contribution is a *static* renormalization of the unstable frequency associated with a stationary bubble.

G. Viscosity corrections to the growth rate

In order to obtain the influence of thermal and quantum fluctuations on the growth rate of the bubble, we must solve the equation of motion (2.47). This is achieved via the Laplace transform. Introducing the Laplace transforms of $Q(t),\Sigma(t)$ as $\tilde{Q}(s),\tilde{\Sigma}(s)$, respectively, with s the Laplace variable. The Laplace transform of Eq. (2.47) with the specified initial conditions is given by

$$\tilde{Q}(s)=\frac{sQ_0}{s^{2}-(\Omega^{2}+\Delta)-\lambda\tilde{\Sigma}(s)}, \tag{2.49}$$

where $\tilde{\Sigma}(s)$ is given by

$$\tilde{\Sigma}(s)=\sum_{p,p'}\frac{|\mathcal{B}_{p,p'}|^{2}}{\omega_p\omega_{p'}}\Bigg\{(1+n_p+n_{p'})\frac{\omega_p+\omega_{p'}}{s^{2}+(\omega_p+\omega_{p'})^{2}}$$
$$-(n_p-n_{p'})\frac{\omega_p-\omega_{p'}}{s^{2}+(\omega_p-\omega_{p'})^{2}}\Bigg\}. \tag{2.50}$$

We now isolate the static contribution by subtracting

$$\tilde{\Sigma}(0)=\lim_{s\to0}\tilde{\Sigma}(s) \tag{2.51}$$

from the Laplace transform of the self-energy. Using the identity

$$\lim_{s\to0}\frac{W}{s^{2}+W^{2}}=\mathcal{P}\left(\frac{1}{W}\right) \tag{2.52}$$

we now fix the counterterm $\delta\Omega^{2}_{ct}$ such that $\Delta+\lambda\tilde{\Sigma}(0)=0$. Introducing

$$\tilde{\Gamma}(s)=\sum_{p,p'}\frac{|\mathcal{B}_{p,p'}|^{2}}{\omega_p\omega_{p'}}\Bigg\{\frac{1+n_p+n_{p'}}{\omega_p+\omega_{p'}}\frac{s^{2}}{s^{2}+(\omega_p+\omega_{p'})^{2}}$$
$$-(n_p-n_{p'})\mathcal{P}\left(\frac{1}{\omega_p-\omega_{p'}}\right)\frac{s^{2}}{s^{2}+(\omega_p-\omega_{p'})^{2}}\Bigg\} \tag{2.53}$$

the Laplace transform of the equation of motion becomes

$$\tilde{Q}(s)=\frac{sQ_0}{s^{2}-\Omega^{2}+\lambda\tilde{\Gamma}(s)}. \tag{2.54}$$

In order to avoid cluttering of notation we will not write explicitly the $\mathcal{P}$ in Eq. (2.53) in what follows, but it must always be understood that the term $1/(\omega_p-\omega_{p'})$ actually refers to its principal part. This principal part prescription

arises from the subtraction in the limit of vanishing s which is the equivalent of the frequency in the real time domain, since the Laplace transform requires that $s \to i\omega + \epsilon$ with ω the frequency [36].

At this stage it becomes clear that the procedure of absorbing the local (zero frequency limit) contributions to the self-energy in the *static* renormalization of the growth rate Ω provides the correct description of the dynamics. Viscosity and dissipative effects only arise from the time dependence of the expectation value of the coordinate and the *static* medium renormalization had already been absorbed into the definition of the growth rate as the limit of zero frequency. Viscosity and dissipation arise from the transfer of energy of the bubble wall to other excitations (mesons) and the growth slows down because of these processes. An important distinction arises in this case as compared to the familiar situation in field theory in which complex poles determine the renormalization to the mass from the *real* part of the self-energy on shell and the decay width from the *imaginary* part of the self-energy on shell. In this case, however, because the frequency associated with the unstable mode is *imaginary*, the real part of the self-energy will renormalize the *growth rate* whereas the imaginary part (if any) at the position of the (purely imaginary pole) will provide *oscillatory* contributions to the bubble dynamics. Therefore, we emphasize that *viscosity* effects that will diminish the growth rate are determined by the *real part of the self-energy* at the position of the pole. This is a striking difference from the usual case in which damping and viscosity are associated with the imaginary part of the self-energy on shell.

The real time dynamics of the bubble growth, $Q(t)$ is given by the inverse Laplace transform

$$Q(t) = \frac{1}{2\pi i}\int_C e^{st}\tilde{Q}(s)ds, \tag{2.55}$$

where $\tilde{Q}(s)$ is given by Eq. (2.54) and C refers to the Bromwich contour running along the imaginary axis to the right of all the singularities of $\tilde{Q}(s)$ in the complex s plane. The analytic structure of $\tilde{Q}(s)$ consists of cuts along the imaginary axis in the s-plane and poles. The two different processes of decay into meson pairs (and recombination) and Landau damping discussed above yield two different cut structures.

The first term in Eq. (2.53) gives a two-meson cut and the contribution from Landau damping determines a cut structure that includes the origin in the s plane. The structure of these cuts depend on the matrix elements of the interaction as well as the full spectrum of excitations and will be investigated in detail for particular cases in the next sections.

The growth rate of the bubble with the quantum fluctuation effects included is given by the pole s_p of $\tilde{Q}(s)$, Eq. (2.54), which satisfies the following relation:

$$s_p^2 - \Omega^2 + \lambda\tilde{\Gamma}(s_p) = 0. \tag{2.56}$$

To first order in λ, the pole of $\tilde{Q}(s)$ which corresponds to a growing bubble is given to lowest order $[\mathcal{O}(\lambda)]$ by

$$s_p = \pm(\Omega + \delta\Omega), \tag{2.57}$$

where the first order quantum and thermal fluctuation correction $\delta\Omega$ to the bubble growth is given by

$$\begin{aligned}\delta\Omega &= -\lambda\frac{\tilde{\Gamma}(\Omega)}{2\Omega}\\ &= -\frac{\lambda}{2}\sum_{p,p'}\frac{|\mathcal{B}_{p,p'}|^2}{\omega_p\omega_{p'}}\Bigg\{\frac{(1+n_p+n_{p'})}{(\omega_p+\omega_{p'})}\\ &\times\left(\frac{\Omega}{\Omega^2+(\omega_p+\omega_{p'})^2}\right) - \frac{n_p - n_{p'}}{\omega_p - \omega_{p'}}\\ &\times\left(\frac{\Omega}{\Omega^2+(\omega_p-\omega_{p'})^2}\right)\Bigg\}.\end{aligned} \tag{2.58}$$

We note that both terms inside bracket in Eq. (2.58) are *positive* since $n_p < n_{p'}$ for $\omega_p > \omega_{p'}$, we recall again that the term $1/(\omega_p - \omega_{p'}) \equiv \mathcal{P}[1/(\omega_p - \omega_{p'})]$ from the discussion following Eq. (2.53). Therefore we conclude that the correction to the growth rate is *negative*, i.e., the dissipative effects of the coupling to mesons results in a smaller growth rate of supercritical bubbles.

Neither the frequencies of oscillations around the stationary bubble nor the matrix elements are quantum mechanical in origin. However, the one loop contribution $\mathcal{O}(\lambda)$ to the self-energy is of quantum origin.

If we restore $\hbar$ in the expression above, this results in $\lambda \to \lambda\hbar$; $T \to T/\hbar$. Obviously neither the eigenvalues of the fluctuation operator nor the matrix elements depend on $\hbar$ but the one loop contribution to the self-energy includes the $\hbar$ from the coupling (one loop) as well as from the temperature factors.

H. Classical limit

In the next sections we will see that the correction to the growth rate is dominated by low lying excitations and for high temperatures these will be such that $\omega_p \ll T$. In this case we can invoke the classical limit which is best understood by restoring $\hbar$ as mentioned above

$$n_k = \frac{1}{e^{\hbar\beta\omega_k} - 1} \approx \frac{T}{\hbar\omega_k} \gg 1. \tag{2.59}$$

In this form,

$$n_k - n_{k'} \approx \frac{T}{\hbar}\left(\frac{1}{\omega_k} - \frac{1}{\omega_{k'}}\right) = -\frac{T}{\hbar}\frac{\omega_k - \omega_{k'}}{\omega_k\omega_{k'}} \tag{2.60}$$

and in the high temperature limit we further approximate

$$1 + n_k + n_{k'} \approx 1 + \frac{T}{\hbar}\frac{\omega_k + \omega_{k'}}{\omega_k\omega_{k'}} \approx \frac{T}{\hbar}\frac{\omega_k + \omega_{k'}}{\omega_k\omega_{k'}}. \tag{2.61}$$

These approximations lead to a simplified expression for the lowest order correction to the growth rate

$$\delta\Omega = -\frac{\lambda T}{2}\sum_{p,p'}\frac{|\mathcal{B}_{p,p'}|^2}{\omega_p^2\omega_{p'}^2} \times\left\{\frac{\Omega}{\Omega^2+(\omega_p+\omega_{p'})^2}+\frac{\Omega}{\Omega^2+(\omega_p-\omega_{p'})^2}\right\}, \tag{2.62}$$

where the product λT is independent of $\hbar$ and displays clearly the classical limit.

The classical limit will be justified in each particular case in the next sections. The expression (2.62) is the final form of the one loop $\mathcal{O}(\lambda)$ correction to the growth rate arising from *dynamical viscosity* since all of the static contributions had been absorbed by the counterterms. This is as far as we can pursue in a general manner without addressing the details of the spectrum of fluctuations around the bubble solution. In the next two sections we study the details of the model determined by the Lagrangian (2.1) with the potential (2.2) for the cases of 1+1 and 3+1 dimensions.

III. THE (1+1)-DIMENSIONAL CASE

As mentioned in the Introduction, the (1+1)-dimensional case is relevant in statistical and condensed matter physics. Quantum field theory models based on the Lagrangian (2.1) with potentials with a stable and metastable state are proposed to describe the low energy phenomenology of quasi-one-dimensional charge density wave systems [12], and therefore their relevance in these physical situations warrants the study of this case.

For $V(\phi)$ given by Eq. (2.2), the solution to the static classical equation of motion (2.9) for one spatial dimension can be found exactly [13,19]. The critical bubble is found to be given by [13,19]

$$\phi_b(x,s_0)=\phi_- +\frac{m}{2\sqrt{2\lambda}}\left\{\tanh\left[\frac{x}{\xi}+s_0\right]-\tanh\left[\frac{x}{\xi}-s_0\right]\right\};$$

$$\xi=\frac{2}{m}, \tag{3.1}$$

where ξ is the width of the bubble wall and s_0 is given in terms of the critical radius R_c by

$$s_0\equiv\frac{R_c}{\xi}\equiv\frac{1}{2}\cosh^{-1}\left(\frac{\epsilon+1}{\epsilon-1}\right) \tag{3.2}$$

with ϵ given by Eq. (2.5). The above solution corresponds to a kink-antikink pair centered at $x=0$, and separated by a distance R_c, and is displayed in Fig. 2. This is the one-dimensional bubble that starts at the false vacuum ϕ_- almost reaches the true vacuum ϕ_+ and returns to ϕ_- and it is similar to the polaron solution found in quasi-one-dimensional polymers [13]. The total energy of the bubble, given by Eq. (2.11), as a function of its dimensionless radius s can be calculated from the field $\phi_b(x,s_0)$ by replacing $s_0=R_c/\xi\rightarrow s=R/\xi$ in Eq. (3.1).

The gradient term $(d\phi_b/dx)^2$ contributes to the surface energy while $V(\phi_b)$ has two contributions; surface contribution and volume contribution. Substituting $V(\phi_b)$ in Eq. (2.11) and evaluating the integral, one finds that the total energy of the bubble is given by

$$E_{\rm var}(s)=E_{\rm sur}(s)+E_{\rm vol}(s) \tag{3.3}$$

with

$$E_{\rm sur}(s)=\frac{-4m^3}{3\lambda}+\frac{4m^3 s}{(-1+e^{4s})\lambda} +\frac{3m^3(-1+e^{8s}-8e^{4s}s)(2+\eta)}{4(-1+e^{4s})^2\lambda} +\frac{4e^{4s}m^3[1-e^{4s}+2(1+e^{4s})s]}{(-1+e^{4s})^3\lambda}, \tag{3.4}$$

$$E_{\rm vol}(s)=-\frac{\eta m^3}{\lambda}s, \tag{3.5}$$

where η is defined as

$$\eta\equiv\sqrt{\epsilon}+\frac{1}{\sqrt{\epsilon}}-2. \tag{3.6}$$

The volume contribution grows linearly with the radius of the bubble while the surface contribution saturates at about the critical radius of the bubble s_0 and attains the following asymptotic value:

$$\lim_{s\rightarrow\infty}E_{\rm sur}(s)\rightarrow\frac{m^3(2+9\eta)}{12\lambda}.$$

In the thin wall limit ($\eta\rightarrow 0$), the surface energy is simply twice the kink mass [35], as the kink-antikink pair became widely separated and the exponential interaction between kink and antikink becomes negligible.

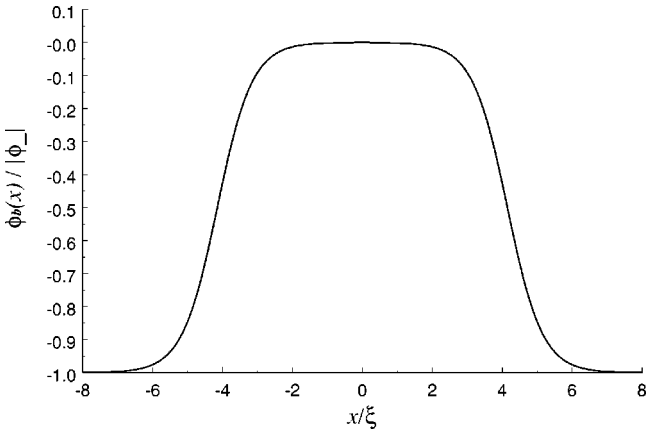

FIG. 2. $\phi_b(x)/|\phi_-|$ for a critical bubble in 1+1 dimensions. $\epsilon=1.001$.

The total energy of the bubble is depicted in Fig. 3. It attains its maximum E_c, at the critical radius s_0 where

$$E_c=\frac{m^3}{24\lambda}[4+12\eta+3\eta^2-3s_0\eta(8+6\eta+\eta^2)] \quad (3.7)$$

with

$$s_0=\frac{1}{2}\cosh^{-1}\left(\frac{\epsilon+1}{\epsilon-1}\right)=\frac{1}{4}\ln\left[\frac{4+\eta}{\eta}\right]. \quad (3.8)$$

In the thin wall limit, the above expressions simplify and we find

$$\eta\simeq\frac{(\epsilon-1)^2}{4}+\mathcal{O}[(\epsilon-1)^3]$$

and

$$E_c=\frac{m^3}{6\lambda}+\mathcal{O}[(\epsilon-1)^2]. \quad (3.9)$$

To study the fluctuations around the bubble solution we need the complete set of eigenfunctions $\{\mathcal{U}_n\}$ satisfying

$$\left[-\frac{d^2}{dx^2}+V''(\phi_b)\right]\mathcal{U}_n(x)=\omega_n^2\mathcal{U}_n(x), \quad (3.10)$$

with

$$V''(\phi_b)=m^2-\frac{3m^2}{2}\mathrm{sech}^2\left[\frac{x}{\xi}+s_0\right]-\frac{3m^2}{2}\mathrm{sech}^2\left[\frac{x}{\xi}-s_0\right].$$

Although the spectrum of eigenfunctions and eigenvalues is known exactly in the case of one kink or antikink [35], for the case of the kink-antikink pair there are not known results that we are aware of. Solving for the eigenfunctions $\{\mathcal{U}_n\}$ in this case is a difficult task but in the thin wall limit, the above potential consists of two identical and widely separated wells centered at $x=\pm R_c$. The spectrum of each potential well is known in the literature [35]. It consists of a zero frequency mode localized in the well, an excited bound state with frequency $3m^2/4$ that is also localized in the well and a continuum of scattering states.

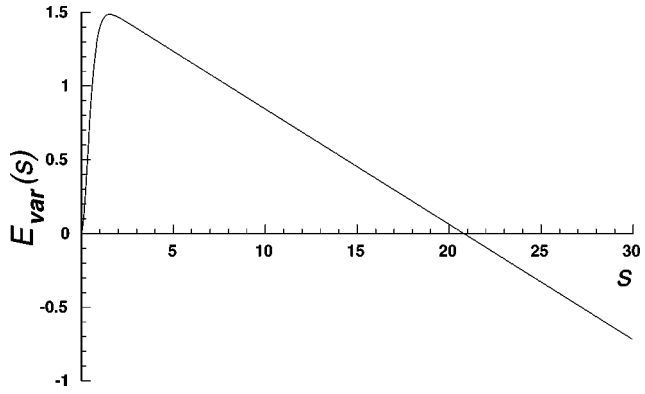

FIG. 3. The total energy of the one dimensional bubble as a function of its dimensionless radius s for $\epsilon=1.2$, $\lambda=0.1$, and $\phi_-=2.0$.

We can use approximate methods such as the linear combination of atomic orbitals approximation (LCAO) (available in elementary textbooks) to provide a reliable estimate for low lying bound states of the above potential from the spectrum of the single potential well. In this method, the ground state of the potential $V''(\phi_b)$ is the *symmetric* linear combination of the ground states of the single well located at $x=\pm R_c$ while the first excited state of $V''(\phi_b)$ is the *antisymmetric* linear combination.

In the thin wall limit, these two states are given by

$$\mathcal{U}_{-1}(x,s_0)=\frac{m}{2\sqrt{E_c}}\frac{d\phi_b}{ds_0}(x,s_0)$$

with

$$\omega_{-1}^2\equiv-\Omega^2\simeq-24m^2e^{-4s_0}=-6\eta m^2 \quad (3.11)$$

and

$$\mathcal{U}_0(x,s_0)=\frac{1}{\sqrt{E_c}}\frac{d\phi_b}{dx}(x,s_0) \quad \text{with} \quad \omega_0^2=0. \quad (3.12)$$

These are the unstable $\mathcal{U}_{-1}$ and the zero $\mathcal{U}_0$ modes which we discussed earlier, see Eqs. (2.19) and (2.21). Obviously $\mathcal{U}_0(x)$ is associated with translations since it is the spatial derivative of the bubble solution and must correspond to a vanishing eigenvalue by translational invariance. Since it is antisymmetric there has to be a nodeless eigenfunction of smaller frequency. The symmetric combination is $\mathcal{U}_{-1}(x)$ and since the two combinations will be split off in energy by a tunneling amplitude that is exponentially small in the distance between the kink and the antikink, the unstable frequency must be negative and exponentially small in this separation as is clearly displayed in Eq. (3.11).

In addition to the unstable and the zero modes, there are two bound states that have energies $\sim(3m^2/4)\pm\Delta E(s_0)$ with energy difference which is again exponentially small in s_0 and correspond to the symmetric and antisymmetric linear combinations of the bound states of the kink in ϕ^4 theory [35] localized at $x=\pm R_c$. Since $V''(\phi_b)$ does not exactly reach m^2 near the center of the bubble, the potential in the Schrödinger equation could allow for shallow bound states near the scattering continuum with binding energies that are exponentially small in the variable s_0. These bound states if present are extremely difficult to obtain.

Finally there is the scattering continuum region of the spectrum characterized by functions $\mathcal{U}_k$, whose eigenfunctions are asymptotically phase shifted plane waves with eigenvalues $\omega_k^2=k^2+m^2$.

In order to compute the matrix elements that enter in the expression for the correction to the growth rate (2.62) we need either the exact form of the eigenfunctions or an excellent approximation to them. Whereas we are confident of our analysis regarding the low lying bound states, we lack a full understanding of shallow bound and continuum states. Such

an understanding requires a detailed study of the spectrum which certainly lies beyond the scope of this article. Although we do not have a complete understanding of the spectrum of eigenfunctions and therefore we do not have even a good approximation to the matrix elements, we can, however, provide some physically reasonable assumptions complemented with dimensional arguments to provide an estimate for the corrections in this case. We begin by noting that in the one kink case, the potential that enters in the Schrödinger equation for the fluctuation is reflectionless [35] and the scattering states for the one kink (or antikink) case have a transmission amplitude which is a pure phase.

Thus we expect that in the thin wall limit when the kink-antikink pair separation is much larger than the width of an isolated kink the wave functions of the scattering states will acquire a phase shift that is at least twice as large as that in the one kink case and will have a rather smooth dependence on the kink-antikink separation. Because the potentials for each kink are reflectionless [35] we *assume* that in the thin wall limit the reflection coefficients of each potential well are very small and therefore there are no substantial interference effects in the region between the kink and the antikink. Under these assumptions the matrix elements $\mathcal{B}_{p,p'}$ will be similar to those calculated in Ref. [41] for a single kink case and fall off very fast at large momenta justifying the classical limit [41]. Hence, under these suitable assumptions the matrix elements are smooth functions of $s_0 = R_c/\xi$. The contribution from the two-meson cut, i.e., the first term in the bracket in Eq. (2.62) is proportional to Ω because the Ω in the denominator can be neglected in comparison with the frequencies for the meson states $\omega_p \approx \mathcal{O}(m)$. Since in 1+1 dimensions the coupling λ has dimensions of $(\text{mass})^2$ the correction to the growth rate arising from the two meson cut is of the form

$$\delta\Omega_{2mes} \approx -\frac{\lambda T}{m^3}\Omega F[s_0] \tag{3.13}$$

with $F[s_0]$ a dimensionless slowly varying function of $s_0 = R_c/\xi$ which is rather difficult to calculate and can only be obtained from a detailed knowledge of the eigenfunctions.

The contribution from the Landau damping cut is more complicated to extract. The second term in the bracket in Eq. (2.62) has the form of a Lorentzian and since Ω is exponentially small it is a function that is strongly peaked at $\omega_p = \omega_{p'}$ and the sum (integral) over p,p' is dominated by a region of width Ω near $\omega_p = \omega_{p'}$. Assuming that the matrix elements are smooth functions of momentum, in this one-dimensional case the integral over a small region $\omega_p - \omega_{p'} \approx \Omega$ can be done by taking a narrow Lorentzian and integrating over the relative momentum within this region [42], leading to a contribution of the form $-(\lambda T/m^2)C[s_0]$, where $C[s_0]$ is a smooth function of its argument that can only be calculated from a detailed knowledge of the scattering wave functions. Hence

$$\delta\Omega_{LD} \approx -\left(\frac{\lambda T}{m^2}\right) C[s_0] \tag{3.14}$$

and the total shift in the frequency is given by $\delta\Omega = \delta\Omega_{2\text{mes}} + \delta\Omega_{LD}$.

Thus we conclude that although we do not have a complete knowledge of the eigenfunctions and therefore cannot provide a complete calculation of the correction to the growth rate, suitable assumptions based on the properties of the spectrum of the one kink case combined with dimensional arguments suggest that to lowest order in the coupling and in the thin wall approximation the growth rate of a slightly supercritical bubble is given by

$$\Omega \approx \frac{4\sqrt{6}}{\xi} e^{-2R_c/\xi}\left[1 - \frac{\lambda T \xi^3}{8} F\left[\frac{R_c}{\xi}\right]\right] - \frac{\lambda T^2 \xi^2}{4} C\left[\frac{R_c}{\xi}\right] + \cdots \tag{3.15}$$

with $F[R_c/\xi], C[R_c/\xi]$ slowly varying dimensionless functions of their argument. Obviously a full calculation of $F[R_c/\xi], C[R_c/\xi]$ requires a detailed understanding of the spectrum, in particular the scattering states. However it is clear from Eq. (3.15) that the validity of a perturbative expansion places a severe constrain on the coupling constant and the value of the temperature, in particular the second contribution in Eq. (3.15) arising from Landau damping gives the leading correction in the thin wall approximation and signals a potential breakdown of perturbation theory in this limit. A more detailed understanding of this possibility requires a better knowledge of the scattering matrix elements, this is an extremely difficult problem that depends on the details of the potential and lies outside the scope of this article.

IV. THE (3+1)-DIMENSIONAL CASE

A. General aspects

We now study the (3+1)-dimensional case which is more relevant from the point of view of particle physics, however, before focusing on a particular form of the potential and bubble profile, we can study fundamental model independent properties of the (3+1)-dimensional case that will determine very robust predictions for the corrections to the bubble growth.

The static bubble configuration $\phi_b(r,R_c)$ is radially symmetric and satisfies the static equation (2.10). To study quantum fluctuations around the critical bubble configuration, we need to find the spectrum of the fluctuation operator $\mathcal{M}$ which in 3 spatial dimensions is given by

$$\mathcal{M} = -\nabla^2 + \left.\frac{\partial^2 V(\phi)}{\partial\phi^2}\right|_{\phi_b(r,R_c)}. \tag{4.1}$$

Since the critical bubble solution is radially symmetric, we write the eigenfunctions $\mathcal{U}_{nlm}(r,\theta,\varphi)$ of the differential operator $\mathcal{M}$ as a product of spherical harmonics $Y_{lm}(\theta,\varphi)$ and radial functions $\psi_{nl}(r)$ that satisfy

$$\left\{-\frac{d^2}{dr^2} - \frac{2}{r}\frac{d}{dr} + \frac{l(l+1)}{r^2} + \frac{\partial^2 V(\phi_b)}{\partial\phi^2}\right\}\psi_{nl}(r) = \omega_n^2 \psi_{nl}(r). \tag{4.2}$$

Because of the translational invariance of the Lagrangian (2.1), there is a three-fold degenerate zero mode given by the eigenfunction $\propto \nabla \phi_b(\vec{x},R_c) \propto Y_{1;\pm 1,0} d\phi_b/dr$ which correspond to translations of the bubble in three dimensions with no energy cost. These are the Goldstone modes of the spontaneously broken translational invariance. This can be easily seen by taking the derivative of Eq. (2.10) with respect to r which results in the following equation:

$$\left\{ -\frac{d^2}{dr^2} - \frac{2}{r}\frac{d}{dr} + \frac{2}{r^2} + \frac{\partial^2 V(\phi_b)}{\partial \phi^2} \right\} \frac{d\phi_b}{dr} = 0. \tag{4.3}$$

In addition to the Goldstone mode, there are other low-lying excitations corresponding to different values of $l \neq 1$. The eigenfunctions of these excitations and their eigenvalues can be obtained by writing the $l=1$ term in the above equation as

$$\frac{2}{r^2} = \frac{l(l+1)}{r^2} - \frac{(l-1)(l+2)}{r^2} \tag{4.4}$$

and we rewrite Eq. (4.3) in the following form:

$$\left\{ -\frac{d^2}{dr^2} - \frac{2}{r}\frac{d}{dr} + \frac{l(l+1)}{r^2} + \frac{\partial^2 V(\phi_b)}{\partial \phi^2} \right\} \frac{d\phi_b}{dr} = \frac{(l-1)(l+2)}{R_c^2} \frac{d\phi_b}{dr} + \delta V(r) \frac{d\phi_b}{dr}, \tag{4.5}$$

where

$$\delta V(r) = (l-1)(l+2)\left[\frac{1}{r^2} - \frac{1}{R_c^2} \right]. \tag{4.6}$$

Since the function $d\phi_b/dr$ is strongly localized at $r=R_c$ in the thin wall limit, the second term on the right hand side is a *small localized perturbation*. Therefore the unperturbed lowest lying eigenvalues are given by

$$\omega_{0l}^2 = \frac{(l-1)(l+2)}{R_c^2}. \tag{4.7}$$

In the thin wall limit, $\xi/R_c \ll 1$ we find that the lowest order correction (in δV) to these eigenvalues is of order $\mathcal{O}(\xi^2/R_c^2)$. For details see Refs. [14,43] and Appendix A. This analysis reveals that there is a band of low lying modes with eigenfunctions

$$\mathcal{U}_{0lm}(r,\theta,\varphi) = \sqrt{N_{0l}} Y_{lm}(\theta,\varphi) \frac{d\phi_b(r,R_c)}{dr} \tag{4.8}$$

with N_{0l} the normalization constants, corresponding to the $(2l+1)$-fold degenerate eigenvalues given by Eq. (4.7). Using Eqs. (2.16), (2.26), (2.21), and (4.7) with $l=0$ (corresponding to the unstable mode) we find the normalization to be given by

$$N_{0l} = \frac{1}{R_c^2 \sigma} \tag{4.9}$$

in terms of the critical radius and the surface tension. We summarize several noteworthy features of these low-lying solutions:

(1) These excitations become Goldstone modes in the limit as $R_c \to \infty$, i.e., in the limit in which the radius of curvature of the bubble goes to infinity. This statement will be understood in detail below in connection with the case of flat interfaces in $3+1$ dimensions.

(2) The eigenfunction with the lowest eigenvalue, corresponds to $l=0$, i.e., a spherically symmetric solution with a negative eigenvalue given by [14,3,43]

$$\omega_{00}^2 \equiv -\Omega^2 = -\frac{2}{R_c^2}. \tag{4.10}$$

This is the unstable mode which corresponds to a spherically symmetric expansion or contraction of the bubble and therefore corresponds to the unstable functional direction. The coordinate associated with this mode is the displacement from the critical radius.

(3) The three Goldstone modes $\mathcal{U}_{0,1,0}; \mathcal{U}_{0,1,\pm 1}$ are the translation modes.

(4) The higher energy modes with $l \geqslant 2$ are excitations on the surface of the bubble, or surface waves with energies given by

$$\omega_{0l}^2 = \frac{(l-1)(l+2)}{R_c^2} = \frac{\Omega^2}{2}(l-1)(l+2); \quad l \geqslant 2. \tag{4.11}$$

These low lying modes will play a dominant role and we will refer to them collectively as $\mathcal{U}_{0lm}$ with eigenvalues given by Eq. (4.7) and whose normalized eigenfunctions Eq. (4.8) are simple functions of the bubble configuration which for the potential (2.2) in the thin wall approximation are given by Eq. (4.27) below.

That the modes with $l \geqslant 2$ can be identified as wiggles of the bubble surface, or surface waves, can be seen from the following expansion [43,44] where as discussed before the translational modes is not included because it is ''clamped'':

$$\begin{aligned} \phi(r,t) &= \phi_b(r-R_c) + q_{-1}(t)\mathcal{U}_{000}(r,\theta,\varphi) \\ &\quad + \sum_{l \geqslant 2;m} a_{lm}(t) Y_{lm}(\theta,\varphi) \left. \frac{d\phi_b}{dr} \right|_{R_c} + \cdots \\ &\simeq \phi_b(r - R(\theta,\varphi,t)) + q_{-1}(t)\mathcal{U}_{000}(r,\theta,\varphi) \\ &\quad + \cdots, \end{aligned} \tag{4.12}$$

where

$$R(\theta,\varphi,t) = R_c - \sum_{l \geqslant 2;m} a_{lm}(t) Y_{lm}(\theta,\varphi).$$

This is an important identification that we emphasize: this band of low-lying modes describes fluctuations of the surface of the bubble. We will argue below that these excitations dominate the infrared behavior of the viscosity correction and will provide the largest contribution to the viscosity coefficient.

The low lying spectrum described above is fairly general and only depends on the existence of a thin wall bubble. Depending on the form of potential $V(\phi)$, there might be other bound states.

An analysis similar to that leading to the band of low-lying excitations reveals that for the potential (2.2) there is another band of rotational bound state excitations that starts near $\omega_{10}^2 \simeq 3m^2/4$. In the thin wall limit the radial wave function for the lowest state in this band is given by the bound state of energy $3m^2/4$ of the ϕ^4 theory in 1+1 dimensions [35] which is also localized at the wall. The eigenfunctions and eigenvalues for this rotational band of excitations are given by (see Appendix A)

$$\mathcal{U}_{1lm}(r,\theta,\varphi) = \sqrt{N_{1l}} Y_{lm}(\theta,\varphi)\psi_1(r);$$

$$\omega_{1l}^2 \approx \frac{3m^2}{4} + \frac{l(l+1)}{R_c^2} + \mathcal{O}\left(\frac{\xi}{R_c}\right), \tag{4.13}$$

where $\psi_1(r)$ is given by the bound state of the theory with potential and (2.2) in one spatial dimension [35], the eigenfunctions in this band are given in Eq. (4.28) below.

Finally there is a continuum of scattering eigenstates with eigenvalues $\omega_k^2 = k^2 + m^2$. As will be discussed later, the contribution to the growth rate from the rotational band (4.13) and of the scattering states is subleading in the thin wall limit. The maximum value of angular momentum available for the low-lying part of the spectrum (4.7) is limited by the edge of the continuum spectrum or the presence of higher bound states, hence $l_{\max}^2/R_c^2 \leqslant m^2$ or $l_{\max}^2 \leqslant (mR_c)^2 = (R_c/\xi)^2$. Therefore in the thin wall limit the maximum value of the angular momentum $l_{\max} \gg 1$.

B. Planar interfaces, surface waves, and (quasi) Goldstone bosons

The low lying spectrum of eigenfunctions given by Eq. (4.8) with eigenvalues (4.7) has a simple physical origin, which can be understood by noticing that in the limit $R_c \to \infty$ the discrete spectrum becomes a continuum. In the limit when the radius of the critical bubble is very large $R_c \to \infty$, the interface between the two phases ϕ_+ and ϕ_- becomes planar and the two phases become degenerate.

Let us consider a static planar interface configuration corresponding to a domain wall along the z axis in three spatial dimensions. Such a configuration satisfies the following equation [35,43]:

$$-\frac{d^2\phi_w(z)}{dz^2} + \frac{\partial V(\phi_w)}{\partial \phi} = 0, \tag{4.14}$$

where $\phi_w(z)$ satisfies the boundary condition $\phi_w(z) \to \phi_\pm$ as $z \to \mp\infty$ and z is the coordinate perpendicular to the planar interface.

The quantum fluctuations around the classical static wall solution $\phi_w(z)$ are given by the spectrum of the differential operator

$$\mathcal{M} = -\nabla^2 + \frac{\partial^2 V[\phi_w(z)]}{\partial \phi^2}. \tag{4.15}$$

Since the domain wall only depends on the coordinate z, the differential operator for the fluctuations is separable in terms of eigenfunctions $\psi_{\vec{q}_\perp}(z,\vec{x}_\perp) = e^{i\vec{q}_\perp\cdot\vec{x}_\perp}\psi_n(z)$, where $\vec{x}_\perp$ denotes the transverse coordinates to z, namely x and y, and $\vec{q}_\perp$ the transverse momentum. The functions $\psi_n(z)$ are solution of the following eigenvalue problem:

$$\left[-\frac{d^2}{dz^2} + \vec{q}_\perp^{\,2} + \frac{\partial^2 V(\phi_w(z))}{\partial \phi^2}\right]\psi_n(z) = \omega_n^2(\vec{q}_\perp)\psi_n(z). \tag{4.16}$$

Taking the derivative of Eq. (4.14) with respect to z, i.e.,

$$\left[-\frac{d^2}{dz^2} + \frac{\partial^2 V(\phi_w)}{\partial \phi^2}\right]\frac{d\phi_w}{dz} = 0 \tag{4.17}$$

and comparing to Eq. (4.15) we see that $d\phi_w/dz$ is the zero mode which corresponds to the translational invariance [35]. Therefore the eigenfunctions

$$\psi_{\vec{q}_\perp} = \exp(i\vec{q}_\perp\cdot\vec{x}_\perp)\frac{d\phi_w}{dz} \tag{4.18}$$

have eigenvalues $\vec{q}_\perp^{\,2}$. These are Goldstone modes associated with translational invariance and represent excitations of the surface of the planar interface $\phi_w(z)$ since

$$\phi(\vec{r}) = \phi_w(z - z_0) + \sum_{q_\perp} a_{q_\perp}\exp(i\boldsymbol{q}_\perp\cdot\boldsymbol{x}_\perp)\frac{d\phi_w}{dz}$$
$$\simeq \phi_w[z - z_\perp(\boldsymbol{x}_\perp)],$$

where z_0 is the position of the planar interface and

$$z_\perp(\boldsymbol{x}_\perp) = z_0 - \sum_{q_\perp} a_{q_\perp}\exp(i\boldsymbol{q}_\perp\cdot\boldsymbol{x}_\perp).$$

This is clearly similar to the case of the spherical bubble Eq. (4.12) and describes the same physics, i.e., fluctuations of the surface. In the case of a planar interface these surface waves are also called capillary waves, and describe the *hydrodynamic* modes of long-wavelength fluctuations of interfaces in systems with two degenerate phases separated by an interface [44]. In the case of degenerate phases, such as, for example, a liquid-gas or an Ising system, these surface waves are Goldstone modes associated with the breakdown of translational invariance by the presence of the interface.

For a spherical bubble in the thin wall limit these surface waves acquire a gap given by the inverse radius (proportional to the Gaussian curvature of the surface). Therefore in analogy with the case of interfaces for degenerate separated phases, we identify these surface fluctuations as quasiGoldstone modes. Since, as argued before the maximum frequency of the surface waves is $<m$ they are *classical* in the high temperature limit $T \gg m$. Hence the surface waves are identified as classical hydrodynamic fluctuations of the bubble shape and quasiGoldstone modes in the thin wall limit.

We want to emphasize that these low energy excitations are a robust feature of the thin wall approximation and are *model independent*. Having studied in detail the *general* aspects of fluctuations around a thin wall bubble, we now focus on the specific details of the theory with a potential given by Eq. (2.2) so as to be able to compute the matrix elements and provide a quantitative analysis of the viscosity effects.

C. ϕ^4 theory: specifics

The critical bubble solution that satisfies Eq. (2.10) with the potential (2.2) is not in general an elementary function, but in the thin wall limit the critical radius of the bubble $mR_c \sim R_c/\xi \gg 1$ and the function $d\phi_b/dr$ is localized near R_c which makes the ''friction'' term, $r^{-1}d\phi_b/dr \propto 1/(mR_c) \sim \xi/R_c \ll 1$. In this limit, the critical bubble solution is found to be

$$\phi_b(r,R_c) = \phi_- + \frac{m}{2\sqrt{2\lambda}}\left\{1-\tanh\left[\frac{r-R_c}{\xi}\right]\right\}; \quad \xi = \frac{2}{m}. \tag{4.19}$$

It corresponds to a field configuration that starts around $r=0$ at the true vacuum ϕ_+, given by Eq. (2.6), and goes to the false vacuum ϕ_- as $r \to \infty$ with a surface width $\xi = m/2$ and a critical radius R_c. Having specified the critical bubble solution ϕ_b, we now go back and determine explicitly the general expressions which we discussed in the previous sections.

The total energy of the bubble as a function of its radius R, given by Eq. (2.11), can be calculated from the field $\phi_b(r,R_c)$ by replacing R_c in Eq. (4.19) by R. The gradient term $(\nabla\phi_b)^2$ contributes to the surface energy while $V(\phi_b)$ has two contributions: a surface contribution $V_s(\phi_b)$ and volume contribution $V_v(\phi_b)$ given by

$$V_s(\phi_b) = \frac{1}{2}[\nabla\phi_b(r)]^2 + \frac{\eta m^4}{32\lambda} \times\left\{\mathrm{sech}^2\left[\frac{r-R}{\xi}\right]\left(3-\tanh\left[\frac{r-R}{\xi}\right]\right)\right\}, \tag{4.20}$$

$$V_v(\phi_b) = -\frac{\eta m^4}{8\lambda}\left(1-\tanh\left[\frac{r-R}{\xi}\right]\right), \tag{4.21}$$

where η is defined by Eq. (3.6). Substituting the above expressions in Eq. (2.11) and evaluating the integral, we find that the total energy of the bubble is given by

$$E_{\mathrm{var}}(R) = \frac{4\pi}{3}V(\phi_+)R^3 + \frac{4\pi R^2 m^3}{12\lambda}\left[1+\frac{9\eta}{2}-\frac{3\eta\xi}{2R} + \left(\frac{\pi^2-6}{12}+\frac{3\pi^2\eta}{8}\right)\frac{\xi^2}{R^2}\right], \tag{4.22}$$

where in the thin wall limit

$$V(\phi_+) \simeq -\frac{\eta m^4}{4\lambda} + \mathcal{O}[(\epsilon-1)^3].$$

The total energy of the bubble is depicted in Fig. 4. It attains its maximum at

$$R_c = \frac{1}{12\xi\eta}[2+9\eta+\sqrt{4+36\eta+45\eta^2}]. \tag{4.23}$$

Using the fact that η is small in the thin wall limit, we find that the critical radius R_c is given by

$$R_c = \frac{1}{3\eta\xi}\{1+\mathcal{O}[(\epsilon-1)^2]\} \to \frac{\xi}{R_c} \simeq 3\eta \tag{4.24}$$

and the total critical energy is given by

$$E_c = \frac{4\pi m}{81\lambda\eta^2}\{1+\mathcal{O}[(\epsilon-1)^2]\} \tag{4.25}$$

which is equivalent to Eqs. (2.13) and (2.14) with the surface tension given by

$$\sigma = \frac{m^3}{12\lambda}. \tag{4.26}$$

The low-lying fluctuation modes $\mathcal{U}_{0lm}(\theta,\varphi,r)$ Eq. (4.8) are given by

$$\mathcal{U}_{0lm}(r,\theta,\varphi) = \frac{\sqrt{6m}}{4R_c}\mathrm{sech}^2\left[\frac{r-R_c}{\xi}\right]Y_{lm}(\theta,\varphi)$$

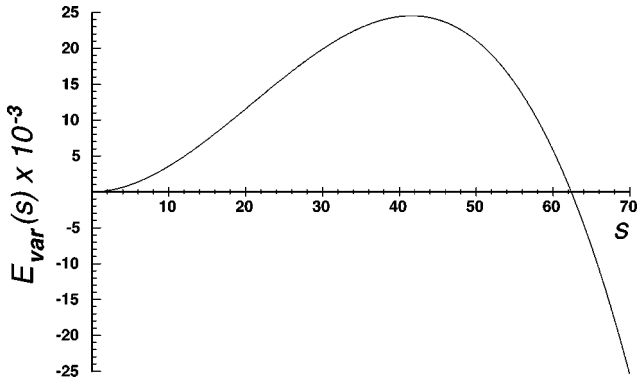

FIG. 4. The total energy of the three dimensional bubble as a function of its dimensionless radius s for $\epsilon=1.2$, $\lambda=0.1$, and $\phi_-=2.0$.

with

$$\omega_{0l}^2=\frac{(l-1)(l+2)}{R_c^2}\left[1+\mathcal{O}\left(\frac{\xi^2}{R_c^2}\right)\right] \tag{4.27}$$

and the next rotational band of bound states is given by (for details see Appendix A)

$$\mathcal{U}_{1lm}(r,\theta,\varphi)\simeq\sqrt{N_{1l}}\,\mathrm{sech}\left[\frac{r-R_c}{\xi}\right]\times\tanh\left[\frac{r-R_c}{\xi}\right]Y_{lm}(\theta,\varphi)$$

with

$$\omega_{1l}^2=\frac{3m^2}{4}+\frac{l(l+1)}{R_c^2}+\mathcal{O}\left(\frac{\xi}{R_c}\right). \tag{4.28}$$

D. Corrections to the bubble growth rate

From Eq. (2.62), the corrections from quantum and thermal fluctuations to the bubble growth in the present case has the following form in the classical limit:

$$\delta\Omega=-\frac{\lambda T}{2}\sum_{qlm,q'l'm'}\frac{|\mathcal{B}_{qlm,q'l'm'}|^2}{\omega_{ql}^2\omega_{q'l'}^2}\times\left\{\frac{\Omega}{\Omega^2+(\omega_{ql}+\omega_{q'l'})^2}+\frac{\Omega}{\Omega^2+(\omega_{ql}-\omega_{q'l'})^2}\right\}, \tag{4.29}$$

where the index q runs over bound and scattering states and

$$\mathcal{B}_{qlm,q'l'm'}\equiv\frac{1}{2\sqrt{\lambda}}\int d^3rV'''(\phi_b)\mathcal{U}_{-1}(r)\mathcal{U}_{qlm}(\mathbf{r})\mathcal{U}_{q'l'm'}(\mathbf{r}) \tag{4.30}$$

with

$$V'''(\phi_b)=-6m\sqrt{2\lambda}\tanh\left[\frac{r-R_c}{\xi}\right]. \tag{4.31}$$

Since V''' is spherically symmetric, the angular integral leads to

$$\mathcal{B}_{qlm,q',l',m'}=\mathcal{B}_{q,q',l}\delta_{l,l'}\delta_{m,m'} \tag{4.32}$$

with

$$\mathcal{B}_{q,q',l}\equiv\frac{(3m)^{3/2}}{4\sqrt{\pi}R_c}\sqrt{N_{ql}}\sqrt{N_{q'l}}\int r^2dr\times\tanh\left[\frac{r-R_c}{\xi}\right]\mathrm{sech}^2\left[\frac{r-R_c}{\xi}\right]\psi_{ql}(r)\psi_{q'l}(r). \tag{4.33}$$

We now note that the bound state energies only depend on l, and that the energy of the scattering states is independent of l. Therefore there is *no Landau damping contribution* from the bound states as consequence of the principal part prescription which subtracts the contribution from $\omega_p=\omega_{p'}$ in the Landau damping term as discussed in detail below Eqs. (2.53),(2.58). Therefore the correction to the growth rate can be written as $\delta\Omega=\delta\Omega_b+\delta\Omega_s$ with the correction from the bound states given by

$$\delta\Omega_b=-\frac{\lambda T}{2}\sum_{n,n'=0,1}\sum_l\frac{(2l+1)|\mathcal{B}_{n,n',l}|^2}{\omega_{nl}^2\omega_{n'l}^2}\times\frac{\Omega}{\Omega^2+(\omega_{nl}+\omega_{n'l})^2} \tag{4.34}$$

and that from the scattering states given by

$$\delta\Omega_s=-\frac{\lambda T}{2}\sum_{k,k'\neq0,1}\sum_l\frac{(2l+1)|\mathcal{B}_{k,k',l}|^2}{\omega_k^2\omega_{k'}^2}\times\left\{\frac{\Omega}{\Omega^2+(\omega_k+\omega_{k'})^2}+\frac{\Omega}{\Omega^2+(\omega_k-\omega_{k'})^2}\right\}. \tag{4.35}$$

The bound state correction has three contributions; the quasiGoldstone modes contribution corresponding to surface waves with $\omega_{0l}^2=\Omega^2(l-1)(l+1)/2$; $l\geqslant2$, the contribution from the higher energy rotational band of bound states near $\omega^2\geqslant3m^2/4$, and the mixed contribution from the quasiGoldstone and the higher energy bound states modes. The denominators in $\delta\Omega_b$ are of order Ω^6 for the quasiGoldstone modes contribution as compared to m^6 for the mixed and the higher energy bound states contributions. Since in the thin wall approximation $m/\Omega\propto R_c/\xi\gg1$, the largest contribution arises from the quasiGoldstone surface modes with the lowest energy denominators. It can be easily seen that the matrix elements cannot compensate for the difference in powers of R_c and that in fact for the higher energy bound states these matrix elements are *smaller* than those for the surface modes because the wave functions $\mathcal{U}_{1lm}$ actually vanish at the position of the bubble wall [see Eq. (4.28)].

The contribution from the scattering states is also seen to be much smaller than that from the surface waves. The frequencies for the continuum states $\omega_k\geqslant m\gg\Omega$ and the two meson cut give a contribution of order Ω (since in the denominators the Ω can be neglected as compared to m). For the Landau damping cut, the argument is similar to that of the case of one space dimension.

For $\Omega\ll m$ this contribution has a Lorentzian shape of width $\approx\Omega$, and the integral over the momenta can be performed in the narrow width approximation. The subtraction of the static contribution guarantees that the integral is dominated by the Lorentzian [42] and the region $\omega_k\approx\omega_{k'}$ can be integrated by changing to relative variables and now in three spatial dimensions the phase space in the region $\omega_k-\omega_{k'}\approx\Omega$ give extra powers of Ω as compared to the one-

dimensional case. Furthermore, the matrix elements are smooth functions of the radius of the bubble as can be understood simply by a scattering argument from a sharply peaked potential in three spatial dimensions. These matrix elements do not introduce any singularity in the limit $R_c/\xi \gg 1$, hence the contribution of the scattering states is at least proportional to Ω and is therefore subleading in the thin wall limit.

This analysis leads to the conclusion that the largest contribution to the correction to the growth rate is given by the *quasiGoldstone modes*, i.e., the surface waves, since these are the lowest lying excitations and hence provide the smallest energy denominators.

The matrix element $\mathcal{B}_{0,0,l}$ for the surface waves can be calculated easily and we find

$$\mathcal{B}_{0,0,l}=\sqrt{\frac{3m}{\pi}}\frac{2}{5R_c^2}=\sqrt{\frac{3m}{\pi}}\frac{\Omega^2}{5} \tag{4.36}$$

leading to the following correction:

$$\delta\Omega_{sw}=-\frac{6\lambda\,\alpha\,mT}{25\pi\ \Omega}, \tag{4.37}$$

where

$$\alpha\equiv\sum_{l=0}^{R_c/\xi}\frac{2l+5}{(l+1)^2(l+4)^2[1+2(l+1)(l+4)]}\simeq 0.039. \tag{4.38}$$

The above series converges rapidly and only the first few terms contribute to the sum, we have evaluated the sum numerically with $R_c/\xi=10$.

Hence we summarize one of the main results of this article: the lowest order correction to the bubble growth for three dimensional bubbles is dominated by viscosity effects arising from the excitation of long-wavelength surface waves and is given by

$$\delta\Omega=-0.003\lambda\,\Omega\,T\xi\left(\frac{R_c}{\xi}\right)^2. \tag{4.39}$$

Therefore to lowest order in λ (one-loop) and to leading order in the thin wall approximation we find that the growth rate of slightly supercritical bubbles is given by

$$\Omega=\frac{\sqrt{2}}{R_c}\left[1-0.003\lambda\,T\xi\left(\frac{R_c}{\xi}\right)^2\right] \tag{4.40}$$

with ξ and R_c are the width and radius of the critical bubble. This is one of the important results of our study. The validity of perturbation theory places a very stringent constraint on the quartic coupling constant in the thin wall limit $R_c/\xi\gg 1$ and in the classical limit $T/m\sim T\xi\gg 1$. The validity of the classical limit in this case is warranted: we are studying the dynamics of nucleation via thermal activation for temperatures below the critical temperature $T<T_c\approx m/\sqrt{\lambda}$ but for temperatures much larger than the energy of the low lying excitations, the relevant regime for thermal activation is $m/\sqrt{\lambda}>T\gg m$ in the weak coupling limit. Furthermore the low-lying excitations with frequencies $\ll m$ are obviously classical.

V. CONCLUSIONS AND DISCUSSION

The focus of this article is to provide a microscopic calculation of the growth rate of slightly supercritical nucleation bubbles. The model under consideration is a ϕ^4 scalar theory with an explicitly symmetry breaking term that produces a metastable and a stable ground state, we studied the case of nucleation in $1+1$ dimensions as well as $3+1$ dimensions. The former is relevant in the case of quasi-one-dimensional charge density wave systems and organic conductors. We begin our analysis by obtaining the critical bubble solution by including finite temperature effects in the potential that enters in the classical equation of motion, counterterms are added to the Lagrangian to compensate for the finite temperature corrections consistently in a perturbative expansion.

Our approach to obtaining the growth rate is very different from previous treatments in that we begin by expanding the quantum field around the critical bubble in terms of the quadratic fluctuations around the critical bubble configuration. These fluctuations describe an unstable direction associated with small departures from the critical radius, translational zero modes, and stable fluctuations. The translational modes are anchored by fixing the center of the bubbles and we treat explicitly the interaction between the coordinate associated with the growth (or collapse) of the bubble with those associated with the stable fluctuations. We obtain the growth rate by obtaining the effective linearized equation of motion for the unstable coordinate by integrating out the coordinates associated with the stable fluctuations. Two different approximations are involved; (i) a weak coupling expansion in terms of λ the quartic self-coupling and (ii) the thin wall approximation in terms of ξ/R_c with ξ the width of the bubble wall and R_c the critical radius. The first approximation allows a consistent perturbative expansion of the self-energy of the unstable coordinate, the second allows a quantitative calculation of the relevant matrix elements, furthermore our analysis reveals that the important fluctuations are *classical* for temperatures $T_c>T\gg m$, with T_c the critical temperature and m the mass of quanta in the metastable phase.

In the one-dimensional case we are able to provide an estimate for the growth rate given by Eq. (3.15) where the functions $F[R_c/\xi], C[R_c/\xi]$ depend in a detailed manner upon the scattering states solutions of the eigenvalue problem for the quadratic fluctuations, and clearly will depend on the details of the potential. This estimate points out the potential breakdown of perturbation theory in the thin wall limit.

In the case of three dimensions we are able to extract some robust features that transcend the form of the potential and are solely a consequence of the thin wall limit. In particular we identify a rotational band of low lying excitations which describe *surface waves*, i.e., ripples on the surface of the bubble. We establish the connection of these surface waves to the capillary waves of flat interfaces in the case of

degenerate but phase separated thermodynamic states (such as the Ising or liquid-gas at coexistence), the surface waves are then identified as *classical long-wavelength hydrodynamic fluctuations*. The unstable coordinate couples to these hydrodynamic fluctuations and as a result the friction term arising from the self-energy is dominated by the coupling to these hydrodynamic modes. Clearly the *coupling* of the unstable coordinate to these hydrodynamic modes depends on the model, and in the case under consideration we find in the thin wall limit and to lowest order in perturbation theory the following expression for the growth rate:

$$\Omega = \frac{\sqrt{2}}{R_c}\left[1 - 0.003\lambda T\xi\left(\frac{R_c}{\xi}\right)^2\right]. \tag{5.1}$$

We also obtain the effective *non-Markovian* Langevin equation for the coordinate describing small departures from the critical radius and establish the generalized fluctuation dissipation relation between the viscosity and the noise kernel. The noise is correlated on time scales comparable to Ω^{-1} precisely as a consequence of the coupling to the hydrodynamic modes and cannot be treated simply with white (delta function) correlations.

Discussion. Although we have studied a specific microscopic model, in the case of $3+1$ dimensions we have been able to identify some robust features that transcend the particular model. These are the existence and dominance of hydrodynamic fluctuations associated with surface waves in the thin wall limit. The coupling of the coordinate associated with small departures from the critical radius to these low energy fluctuations induces friction or viscosity corrections to the growth rate of slightly supercritical bubbles and in the weak coupling and thin wall limit these fluctuations give the largest contribution to the friction corrections.

One of our original motivations is to make contact with previous studies of nucleation as applied to the quark-hadron phase transition. In particular Csernai and Kapusta [3] have parametrized the coarse grained free energy that describes a quark-hadron first order phase transition in terms of a local energy variable that can be identified with our scalar field ϕ. The form of the potential taken by these authors coincides with our potential $V(\phi)$ (2.2), with coefficients that depend on temperature, just as we have argued in this article. Their form of the critical bubble solution and the variational energy as a function of the radius of a bubble are very similar to those studied in this article. These authors have established that for about 1% supercooling the critical radius for such a model is about $R_c \approx 12\,\mathrm{fm}$, the width of the wall is about $\xi \approx 0.7\,\mathrm{fm}$, and the thin wall approximation must be reliable in this regime.

We can obtain the quartic self-coupling λ in Eq. (2.2) from the parameters used in Ref. [3] by relating the width of the bubble $\xi = 2/m$ and the surface tension σ to λ via Eq. (4.26). In Ref. [3] the value of the surface tension for the particular quark-hadron model is $\sigma = 50\,\mathrm{MeV/fm^2}$ for $T \approx 200\,\mathrm{MeV}$, yielding a value $\lambda \approx 6$ which leads to a very large correction to the growth rate. Certainly the large value of the coupling invalidates the perturbative scheme and we cannot draw a definite conclusion as to the relevance of our lowest order estimate for the quark-hadron transition beyond the statement that the viscosity induced by the hydrodynamic fluctuations *could* result in a very large (negative) correction to the growth rate and therefore a rather small nucleation rate.

For larger supercooling the critical radius becomes smaller and the thin wall approximation breaks down, but in this case nucleation and spinodal decomposition will be indistinguishable and homogenous nucleation theory may not be the proper description.

However, despite the limitations of the perturbative expansion and the thin wall approximation, we have provided a consistent approach to obtain friction or viscosity corrections to the growth rate from a *microscopic* perspective without invoking a phenomenological description. The observation that in the thin wall limit the most important corrections arise from the coupling to *classical* hydrodynamic fluctuations could perhaps pave the way to a systematic hydrodynamic treatment that would circumvent the weak coupling expansion and allow us to extract nonperturbative physics.

VI. ACKNOWLEDGMENTS

D.B. thanks the N.S.F for partial support through the grants PHY-9605186 and INT-9512798. S.M.A. thanks King Fahad University of Petroleum and Minerals (Saudi Arabia) for financial support. S.E.J. thanks CNPq for financial support. F.I.T. thanks FAPEMIG for support. E.S.F. thanks CNPq and FAPERJ for support and D.G.B. thanks FAPERJ and CNPq for support through a binational collaboration.

APPENDIX A: CORRECTIONS TO THE QUASIGOLDSTONE MODES

In this appendix we calculate the corrections to the eigenvalues of the quasiGoldstone modes that obey the Eq. (4.5) using first order perturbation theory. First we write

$$\frac{(l-1)(l+2)}{r^2} = \frac{(l-1)(l+2)}{R_c^2} + \delta V \tag{A1}$$

with

$$\delta V = (l-1)(l+2)\left(\frac{1}{r^2} - \frac{1}{R_c^2}\right).$$

The first order energy correction $E_l^{(1)}$ is given by

$$E_l^{(1)} = -\langle \mathcal{U}_{0lm}|\,\delta V|\mathcal{U}_{0lm}\rangle = -\frac{(l-1)(l+2)}{R_c^2}\int_0^\infty r^2 dr N_{0l}\left(\frac{d\phi_b}{dr}\right)^2\left(\frac{R_c^2}{r^2} - 1\right), \tag{A2}$$

where we have integrated out the angular degrees of freedom.

For the ϕ^4 potential given by Eq. (2.2), the normalized wave functions are given by Eq. (4.27) and when it is substituted in Eq. (A2) one finds that

$$E_l^{(1)}=\frac{(l-1)(l+2)}{R_c^2}\,\frac{(\pi^2-6)}{12}\,\frac{\xi^2}{R_c^2};\quad \xi=\frac{2}{m}. \tag{A3}$$

Thus to first order in perturbation theory, the eigenvalues are given by

$$\omega_{0l}^2=\frac{(l-1)(l+2)}{R_c^2}\left[1+\mathcal{O}\left(\frac{\xi^2}{R_c^2}\right)\right].$$

A similar treatment can be used for the next rotational band based on the bound state of the ϕ^4 theory in one spatial dimension. For this we treat the term

$$\delta V^{(1)}=-\frac{2}{r}\frac{d}{dr}+l(l+1)\left[\frac{1}{R_c^2}-\frac{1}{r^2}\right] \tag{A4}$$

as a perturbation. The unperturbed wave function is the positive energy bound state of the one-dimensional ϕ^4 theory [35] and the first order correction is obtained as before and is $l(l+1)/R_c^2+\mathcal{O}(\xi/R_c)$.

APPENDIX B: LANGEVIN EQUATION AND FLUCTUATION DISSIPATION RELATION

The semiclassical Langevin equation is obtained by performing the path integrals over the bath degrees of freedom, i.e., the stable modes, thus obtaining a nonequilibrium effective functional for the unstable mode. This is achieved consistently in perturbation theory [39,41], and to lowest order we find

$$Z[j^+=j^-=0]=\int \mathcal{D}q_{-1}^+\mathcal{D}q_{-1}^-e^{i\int_{-\infty}^{\infty}dt'(L_0[q_{-1}^+]-L_0[q_{-1}^-])}\mathcal{F}[q_{-1}^+,q_{-1}^-], \tag{B1}$$

where the Lagrangians $L_0[q_{-1}^{\pm}]$ are given by Eq. (2.30) and $\mathcal{F}[q_{-1}^+,q_{-1}^-]$ is the influence functional [45,46] which to one loop order and neglecting the tadpole contributions is given by

$$\begin{aligned}\mathcal{F}[q_{-1}^+,q_{-1}^-]=&\exp\Bigg\{-i^2\lambda\sum_{p,p'}|\mathcal{B}_{pp'}|^2\int dtdt'\\&\times[q_{-1}^+(t)G_p^{++}(t,t')G_{p'}^{++}(t,t')q_{-1}^+(t')\\&+q_{-1}^-(t)G_p^{--}(t,t')G_{p'}^{--}(t,t')q_{-1}^-(t')\\&-q_{-1}^+(t)G_p^{+-}(t,t')G_{p'}^{+-}(t,t')q_{-1}^-(t')\\&-q_{-1}^-(t)G_p^{-+}(t,t')G_{p'}^{-+}(t,t')q_{-1}^+(t')]\Bigg\},\end{aligned} \tag{B2}$$

where the Green's functions are given by Eq. (2.43).

Introducing the Wigner coordinates or center of mass and relative coordinates, $x(t)$ and $r(t)$, respectively, given by

$$x(t)=\frac{1}{2}[q_{-1}^+(t)+q_{-1}^-(t)],\quad r(t)=q_{-1}^+(t)-q_{-1}^-(t),$$

the generating functional becomes [46–50]

$$Z[0]=\int \mathcal{D}x\mathcal{D}re^{iS[x,r]} \tag{B3}$$

with the nonequilibrium effective action given by

$$\begin{aligned}S[x,r]=\int dtr(t)\Bigg[&-\ddot{x}(t)+\Omega^2x(t)+\lambda\int dt'\\&\times\left(\Sigma_{\rm ret}(t-t')x(t')+\frac{i}{2}K(t-t')r(t')\right)\Bigg],\end{aligned} \tag{B4}$$

where for clarity we have neglected the counterterms as well as the tadpoles arising in the computation of the influence functional. The kernels $\Sigma_{\rm ret}(t-t')$ and $K(t-t')$ are given by

$$\Sigma_{\rm ret}(t-t')=\Sigma(t-t')\Theta(t-t'),$$

$$\begin{aligned}K(t-t')=&-\sum_{p_1,p_2}|\mathcal{B}_{p_1p_2}|^2\{\mathcal{G}_{p_1}^{>}(t,t')\mathcal{G}_{p_2}^{>}(t,t')\\&+\mathcal{G}_{p_1}^{<}(t,t')\mathcal{G}_{p_2}^{<}(t,t')\}\\=&\sum_{p,p'}\frac{|\mathcal{B}_{pp'}|^2}{2\omega_p\omega_{p'}}\{(1+n_p+n_{p'}+2n_pn_{p'})\\&\times\cos[(\omega_p+\omega_{p'})(t-t')]\\&+(n_p+n_{p'}+2n_pn_{p'})\cos[(\omega_p-\omega_{p'})(t-t')]\},\end{aligned} \tag{B5}$$

with $\Sigma(t-t')$ given by Eq. (2.48).

At this stage it proves convenient to introduce the identity

$$e^{-(1/2)\int dtdt'r(t)K(t-t')r(t')}=C(t)\int \mathcal{D}\xi e^{-(1/2)\int dtdt'\xi(t)K^{-1}(t-t')\xi(t')+i\int dt\xi(t)r(t)}$$

with C(t) being an inessential normalization factor, to cast the nonequilibrium effective action of the unstable mode in terms of a stochastic noise variable with a definite probability distribution, [46–50]. Using the above relation, the generating functional becomes

$$\begin{aligned}Z[0]=\int \mathcal{D}x\mathcal{D}r\mathcal{D}\xi P[\xi]\exp\Bigg\{i\int dtr(t)\Bigg[&-\ddot{x}(t)+\Omega^2x(t)\\&+\lambda\int_{-\infty}^{t}dt'\Sigma(t-t')x(t')+\xi(t)\Bigg]\Bigg\},\end{aligned} \tag{B6}$$

where the probability distribution of the stochastic noise $P[\xi]$ is given by

$$P[\xi]=\int \mathcal{D}\xi \exp\left\{-\frac{1}{2\lambda}\int dt dt' \xi(t)K^{-1}(t-t')\xi(t')\right\}. \tag{B7}$$

In this approximation we find that the noise-noise correlation function is given by

$$\langle\langle \xi(t)\xi(t')\rangle\rangle = K(t-t'), \tag{B8}$$

which is in general colored, i.e., it is not a delta function $\delta(t-t')$.

The semiclassical Langevin equation is obtained by extremizing the effective action in Eq. (B6) with respect to $r(t)$

$$\ddot{x}(t)-\Omega^2 x(t)-\lambda\int_{-\infty}^{t} dt' \Sigma(t-t')x(t')=\xi(t). \tag{B9}$$

Taking the average of the above equation with the noise probability distribution $P[\xi]$ and identifying $\langle\langle x(t)\rangle\rangle = Q(t)$ yields the equation of motion for the expectation value of the unstable mode, Eq. (2.47).

The relationship between the kernels $\Sigma_{\rm ret}(t-t')$ and $K(t-t')$ constitutes a generalized quantum fluctuation dissipation relation. This relation is established by considering the time Fourier transforms of the functions $\mathcal{G}^{>}_{p}(t,t')\mathcal{G}^{>}_{p'}(t,t')$ and $\mathcal{G}^{<}_{p}(t,t')\mathcal{G}^{<}_{p'}(t,t')$ which are denoted by $\mathcal{G}^{>}_{pp'}(\omega)$ and $\mathcal{G}^{<}_{pp'}(\omega)$, respectively. These Fourier transforms obey the KMS condition [51]

$$\mathcal{G}^{<}_{pp'}(\omega)=e^{-\beta\omega}\mathcal{G}^{>}_{pp'}(\omega). \tag{B10}$$

Using the above relation we find that $\Sigma_{\rm ret}(\omega)$, the Fourier transform in time of the retarded self-energy $\Sigma_{\rm ret}(t-t')$ is given by

$$\Sigma_{\rm ret}(\omega)=2\sum_{p,p'}|\mathcal{B}_{pp'}|^2\int\frac{d\omega'}{2\pi}\frac{\mathcal{G}^{>}_{pp'}(\omega')[1-e^{-\beta\omega'}]}{\omega-\omega'+i\epsilon}, \tag{B11}$$

leading to the imaginary part

$$\mathrm{Im}[\Sigma_{\rm ret}(\omega)]=-(1-e^{-\beta\omega})\sum_{p,p'}|\mathcal{B}_{pp'}|^2\mathcal{G}^{>}_{pp'}(\omega). \tag{B12}$$

On the other hand the kernel that determines the noise-noise correlation function $K(t-t')$ has a Fourier transform given by $k(\omega)$ with

$$\begin{aligned} k(\omega)&=(1+e^{-\beta\omega})\sum_{p,p'}|\mathcal{B}_{pp'}|^2\mathcal{G}^{>}_{pp'}(\omega)\\ &=-\coth\left[\frac{\beta\omega}{2}\right]\mathrm{Im}[\Sigma_{\rm ret}(\omega)]. \end{aligned} \tag{B13}$$

The above relation between the Fourier transform of the noise-noise correlation function and the imaginary part of the self-energy is the generalized fluctuation-dissipation relation.

In particular the contribution from the surface waves to the kernel $K(t-t')$ is given by

$$K_{sw}(\tau)=\frac{12mT^2}{25\pi}\sum_{l\geqslant 2}^{R_c/\xi}\frac{(2l+1)}{(l-1)^2(l+2)^2}\times\left\{1+\cos\left[2\sqrt{(l-1)(l+2)}\frac{\tau}{R_c}\right]\right\}. \tag{B14}$$

This function oscillates with constant amplitude on a time scale $\sim R_c$ which is the same time scale for growth of a supercritical bubble. Therefore the noise term *cannot* be taken to be uncorrelated over the time scales associated with the growth of a bubble, i.e., the noise is *colored* and a Langevin description based on a white noise would miss the long-time correlations. The contribution of the scattering states *could* lead to a short range part of the kernel, but the long time behavior of the kernel will be dominated by the low energy surface waves. The reason that a Markovian Langevin equation with white noise fails to describe the dynamics of the unstable coordinate is that there are slow hydrodynamic fluctuations with time scales comparable to the growth rate that couple to the unstable coordinate, precisely the same type of fluctuations that dominate the viscosity or friction.

[1] E. V. Shuryak, Phys. Rep. **61**, 71 (1980); H. Stöcker and W. Greiner, *ibid.* **137**, 277 (1986); B. Muller, *The Physics of the Quark Gluon Plasma,* Vol. 225 of *Lecture Notes in Physics* (Springer-Verlag, Berlin, 1985); L. P. Csernai, *Introduction to Relativistic Heavy Ion Collisions* (Wiley, England, 1994); C. Y. Wong, *Introduction to High-Energy Heavy Ion Collisions* (World Scientific, Singapore, 1994).

[2] For a comprehensive review of aspects of the QCD phase transition see H. Meyer-Ortmanns, Rev. Mod. Phys. **68**, 473 (1996).

[3] L. P. Csernai and J. I. Kapusta, Phys. Rev. D **46**, 1379 (1992); L. P. Csernai and J. I. Kapusta, Phys. Rev. Lett. **69**, 737 (1992); M. Carrington and J. I. Kapusta, Phys. Rev. D **47**, 5304 (1993).

[4] A. G. Cohen, D. B. Kaplan, and A. E. Nelson, Annu. Rev. Nucl. Part. Sci. **43**, 27 (1993); Phys. Lett. B **263**, 86 (1991); **295**, 57 (1992); Nucl. Phys. **B349**, 727 (1991).

[5] V. A. Rubakov and M. E. Shaposhnikov, Phys. Usp. **39**, 461 (1996); G. R. Farrar and M. E. Shaposhnikov, Phys. Rev. D **50**, 774 (1994); V. A. Kuzmin, V. A. Rubakov, and M. E. Shaposhnikov, Phys. Lett. **155B**, 36 (1985); G. Farrar, Nucl. Phys. B (Proc. Suppl.) **43**, 312 (1995); M. E. Shaposhnikov, Phys. Lett. B **277**, 324 (1992).

[6] For a review of possible mechanisms for Baryogeneis see A. Dolgov, Phys. Rep. **222**, 309 (1992); N. Turok, *Electroweak Baryogenesis*, in *Perspectives on Higgs Physics*, edited by G. L. Kane (World Scientific, Singapore, 1993), p. 300; M. Trodden, ''Electroweak Baryogenesis,'' hep-ph/9803479; A. Riotto, ''Theories of Baryogenesis,'' hep-ph/9807454.

[7] A. Linde, *Particle Physics and Inflationary Cosmology* (Har-

wood Academic Publishers, Switzerland, 1990); Rep. Prog. Phys. **47**, 925 (1984).
[8] E. W. Kolb and M. S. Turner, *The Early Universe* (Addison Wesley, Reading, MA, 1990).
[9] R. Brandenberger, Rev. Mod. Phys. **57**, 1 (1985); Int. J. Mod. Phys. A **2**, 77 (1987).
[10] For a review of nucleation in soft condensed matter physics see J. D. Gunton, M. San Miguel, and P. S. Sahni, in *Phase Transitions and Critical Phenomena*, edited by C. Domb and J. L. Lebobowitz (Academic Press, London, 1983), Vol. 8.
[11] J. S. Langer and K. Binder, in *Systems Far from Equilibrium*, Vol. 132 of Lecture Notes in Physics, edited by L. Carrido (Springer-Verlag, Sitges, 1980).
[12] Yu-Lu, *Solitons and Polarons in Conducting Polymers* (World Scientific, Singapore, 1988); A. J. Heeger, S. Kivelson, J. R. Schrieffer, and W. P. Su, Rev. Mod. Phys. **60**, 781 (1988); G. Grüner, *Density Waves in Solids* (Addison-Wesley, 1994).
[13] D. Boyanovsky, C. A. A. de Carvalho, and E. S. Fraga, Phys. Rev. B **50**, 2889 (1994); C. A. A. de Carvalho, Acta Phys. Pol. B **19**, 875 (1988); Mod. Phys. Lett. B **3**, 125 (1989); E. S. Fraga and C. A. A. de Carvalho, Phys. Rev. B **52**, 7448 (1995); D. G. Barci, E. S. Fraga, and C. A. A. de Carvalho, Phys. Rev. D **55**, 4947 (1997).
[14] J. S. Langer, Ann. Phys. (N.Y.) **41**, 108 (1967); **54**, 258 (1969); **65**, 53 (1971); J. S. Langer and L. A. Turski, Phys. Rev. A **8**, 3230 (1973); L. A. Turski and J. Langer, *ibid.* **22**, 2189 (1980).
[15] S. Coleman, Phys. Rev. D **15**, 2929 (1977); C. Callan and S. Coleman, *ibid.* **16**, 1762 (1977).
[16] M. Stone, Phys. Lett. **76B**, 186 (1977).
[17] I. Affleck, Phys. Rev. Lett. **46**, 388 (1981).
[18] A. D. Linde, Nucl. Phys. **B216**, 421 (1983). There is a factor proportional to the growth rate of a supercritical bubble missing in the pre-exponential factor in this article, see Refs. [14,17,3].
[19] D. Boyanovsky and C. A. A. de Carvalho, Phys. Rev. D **48**, 5850 (1993).
[20] L. Carson, X. Li, L. McLerran, and R. T. Wang, Phys. Rev. D **42**, 2127 (1990).
[21] J. Baacke, Phys. Rev. D **52**, 6760 (1995); J. Baacke and S. Junker, *ibid.* **49**, 2055 (1994); J. Baacke and V. Kiselev, **48**, 5648 (1993).
[22] M. Gleiser, G. C. Marques, and R. O. Ramos, Phys. Rev. D **48**, 1571 (1993); G. H. Flores, R. O. Ramos, and N. F. Svaiter, Int. J. Mod. Phys. A **14**, 3715 (1999).
[23] F. Ruggeri and W. A. Friedman, Phys. Rev. D **53**, 6543 (1996).
[24] J. I. Kapusta and A. P. Vischer, Phys. Rev. C **52**, 2725 (1995); J. I. Kapusta, A. P. Vischer, and R. Venugopalan, *ibid.* **51**, 901 (1995).
[25] E. E. Zabrodin, L. V. Bravina, H. Stöcker, and W. Greiner, Phys. Rev. C **59**, 894 (1999); E. E. Zabrodin, L. V. Bravina, L. P. Csernai, H. Stöcker, and W. Greiner, Phys. Lett. B **423**, 373 (1998).
[26] D. Chandra and A. Boyal, hep-ph/9903466.
[27] A. Strumia and N. Tetradis, hep-ph/9904246.
[28] J. Ignatius, in *Strong and Electroweak Matter '97*, edited by F. Csikor and Z. Fodor (World Scientific, Singapore, 1998).
[29] S. Y. Khlebnikov, Phys. Rev. D **46**, 3223 (1992).
[30] P. Arnold, Phys. Rev. D **48**, 1539 (1993).
[31] J. Borrill and M. Gleiser, Phys. Rev. D **51**, 4111 (1995); M. Gleiser, Phys. Rev. Lett. **73**, 3495 (1994); M. Alford and M. Gleiser, Phys. Rev. D **48**, 2838 (1993); M. Gleiser, G. C. Marques, and R. O. Ramos, *ibid.* **48**, 1571 (1993); M. Gleiser, A. F. Heckler, and E. W. Kolb, Phys. Lett. B **405**, 121 (1997); M. Gleiser and A. F. Heckler, Phys. Rev. Lett. **76**, 180 (1996).
[32] R. Haas, Phys. Rev. D **57**, 7422 (1998).
[33] B. H. Lin, L. McLerran, and N. Turok, Phys. Rev. D **46**, 2668 (1992).
[34] Y. Brihaye and J. Kunz, Phys. Rev. D **48**, 3884 (1993).
[35] R. Rajaraman, *Kinks and Instantons An Introduction to Kinks and Instantons in Quantum Field Theory* (North-Holland Publishing, Amsterdam, 1982).
[36] D. Boyanovsky and H. J. de Vega, Phys. Rev. D **47**, 2343 (1993); D. Boyanovsky, D. S. Lee, and Anupam Singh, *ibid.* **48**, 800 (1993); D. Boyanovsky, M. D'Attanasio, H. J de Vega, R. Holman, and D. S. Lee, *ibid.* **52**, 6805 (1995).
[37] D. Boyanovsky, H. J. de Vega, R. Holman, and M. Sinionato, Phys. Rev. D **60**, 065003 (1999).
[38] J. Schwinger, J. Math. Phys. **2**, 407 (1961); L. V. Keldysh, Zh. Eksp. Teor. Fiz. **47**, 1515 (1964) [Sov. Phys. JETP **20**, 1018 (1965)]; K. T. Mahanthappa, Phys. Rev. **126**, 329 (1962); P. M. Bakshi and K. T. Mahanthappa, J. Math. Phys. **4**, 1 (1963); **4**, 12 (1963); V. Korenman, Ann. Phys. (N.Y.) **39**, 72 (1966); G. Z. Zhou, Z. B. Su, B. L. Hao, and L. Yu, Phys. Rep. **118**, 1 (1985); J. Rammer and H. Smith, Rev. Mod. Phys. **58**, 323 (1986); E. M. Lifshitz and L. P. Pitaevskii, *Physical Kinetics* (Pergamon, New York, 1981); G. D. Mahan, *Many Particle Physics*, 2nd ed. (Plenum, New York, 1990); H. Kleinert, *Path Integrals in Quantum Mechanics, Statistics and Polymer Physics*, 2nd ed. (World Scientific, Singapore, 1996); R. Mills, *Propagators for Many Particle Systems* (Gordon and Breach, New York, 1969).
[39] D. Boyanovsky, H. J. de Vega, R. Holman, D.-S. Lee, and A. Singh, Phys. Rev. D **51**, 4419 (1995); D. Boyanovsky, H. J. de Vega, and R. Holman, *Proceedings of the Second Paris Cosmology Colloquium*, Observatoire de Paris, June 1994, edited by H. J. de Vega and N. Sánchez (World Scientific, Singapore, 1995) pp. 127–215; *Advances in Astrofundamental Physics*, Erice Chalonge School, edited by N. Sánchez and A. Zichichi (World Scientific, Singapore, 1995); D. Boyanovsky, H. J. de Vega, and R. Holman, *Vth. Erice Chalonge School, Current Topics in Astrofundamental Physics*, edited by N. Sánchez and A. Zichichi (World Scientific, Singapore, 1996), pp. 183–270.
[40] H. A. Weldon, Phys. Rev. D **28**, 2007 (1983).
[41] S. M. Alamoudi, D. Boyanovsky, and F. Takahura, Phys. Rev. D **58**, 105003 (1998); Phys. Rev. B **57**, 919 (1998).
[42] We thank Peter Arnold for an illuminating discussion on this point.
[43] N. J. Günther, D. A. Nicole, and D. J. Wallace, J. Phys. A **13**, 1755 (1980); D. J. Wallace, in *Recent Advances in Field Theory and Statistical Mechanics*, edited by J-B. Zuber and R. Stora (North-Holland Publishing Co., Amsterdam, 1984).
[44] S. A. Safran, *Statistical Thermodynamics of Surfaces, Interfaces and Membranes* (Addison Wesley, New York, 1994).
[45] R. Feynman and F. Vernon, Ann. Phys. (N.Y.) **24**, 118 (1963).
[46] A. O. Caldeira and A. J. Leggett, Physica A **121**, 587 (1983).

[47] A. Schmid, J. Low Temp. Phys. **49**, 609 (1982).
[48] H. Grabert, P. Schramm, and G.-L. Ingold, Phys. Rep. **168**, 115 (1988).
[49] U. Weiss, *Quantum Dissipative Systems* (World Scientific, Singapore, 1993), and references therein.
[50] D. Boyanovsky and D.-S. Lee, Nucl. Phys. **B**[FS] **406**, 631 (1993).
[51] A. L. Fetter and J. D. Walecka, *Quantum Theory of Many Particle Systems* (McGraw-Hill, San Francisco, 1971), Chap. 9.